As originally published in the SMTA Proceedings.

A Collaborative Consortia Project to Assess the Effect of Thermal Cycling Dwell Time on the Reliability of High- Performance Solder Alloys

Richard Coyle, Dave Hillman, Tim Pearson, Michael Osterman, Joe Smetana, Keith Howell, Julie Silk, Hongwen Zhang, Jie Geng, Derek Daily, Anna Lifton, Morgana Ribas, Raiyo Aspandiar, Faramarz Hadian, Chloe Feng, Ranjit Pandher, Jayse McLean, James Wertin, Babak Arfaei, Jean-Christophe Riou, Madan Jagernauth, Denny Fritz, Shantanu Joshi, Jasbir Bath, Stuart Longgood, and Andre Kleyner

richard.coyle@nokia-bell-labs.com

ABSTRACT

The past decade has seen the development and introduction of commercial, third-generation, high-performance Pb-free solder alloys designed to meet the requirements of higher temperature use environments. Most of these offerings are based on the Sn-Ag-Cu (SAC) system, with major alloying additions of bismuth (Bi), antimony (Sb), or Indium (In). These elements, individually or in combination, promote additional precipitate, solid solution, or dispersion strengthening that can enhance resistance to degradation at elevated temperature or during aggressive thermal cycling. Results from the literature show that an increase in thermal cycling dwell time can decrease the thermal cycling reliability of SAC solders. Because high-performance alloys are designed for extended operation at higher temperatures, it is important to characterize their reliability at extended thermal cycling dwell times. This paper describes the planning and progress of the experimental program designed to assess the effect of a 60-minute temperature cycling dwell time on the thermal fatigue performance and microstructure of third generation, high-performance Pb-free solder alloys.

Key words: Pb-free solder, high-performance solder alloys, thermal fatigue, thermal cycling, dwell time, solder microstructure

INTRODUCTION

Significant advancements have been made in Pb-free solder alloy development since the implementation of the RoHS Directive in 2006 [1]. Alloy advancement continues to be driven primarily by experience gathered through volume manufacturing and increased deployment of a variety of Pb-free products of increasing complexity. Consequently, Pb-free solder alloy offerings have increased in number and metallurgical complexity, well beyond the various commercial near-eutectic Sn-Ag-Cu (SAC) alloys that replaced eutectic SnPb solder [2]. This trend includes the emergence of a family of third generation, high-performance alloys designed to address reliability requirements for increasingly more aggressive use environments [3]. These alloys are based on the SAC system but substitute major alloying additions of bismuth (Bi), antimony (Sb), or indium (In) for tin (Sn).

Resistance to thermal fatigue damage is required for the products of many high reliability end users [4]. Solder joints age and degrade during service and eventually fail by the common wear out mechanism of thermally activated solder creep-fatigue or simply thermal solder fatigue [5]. Solder fatigue is the major wear-out failure mode and major source of failure for surface mount (SMT) components in electronic assemblies [6].

From 2008 to 2015, the Pb-Free Alloy Alternatives Project, sponsored by the International Electronics Manufacturing Initiative (iNEMI) planned and executed test programs to close knowledge gaps related to thermal fatigue performance of Sn-based, Pb free solder alloys [2, 4, 7-21]. Most of the alloys studied in the Alloy Alternatives Project had near-eutectic SAC compositions. In 2016, a new phase of the project was launched to characterize and understand the thermal fatigue performance of the emerging high-performance Pb-free solder alloys. The new project phase uses the thermal cycling practices and test vehicles developed for the original iNEMI Alloy study to generate data for high-performance solder alloys [22].

The Alloy Alternatives project team was created by a formal collaboration between iNEMI and another major industrial consortium, the HDP User Group, and includes participation from two other consortia, the CALCE (Center for Advanced Life Cycle Engineering), and AREA (Universal Advanced Research in Electronic Assembly). These consortia collectively are supported by members from high reliability telecom, automotive, avionics, and military/defense end users, solder suppliers, and electronic contract manufacturers.

The temperature cycling profiles for evaluating high-performance alloys were selected to address the requirements of three specific industries or market segments. Telecom is represented by TC1 (0/100 °C), consumer/handheld and automotive qualification by TC4 (-40/125 °C) and

aerospace/defense by TC7 (-55/125 °C). These are defined in Table 4-1 from IPC-9701B [23], which specifies nominal low and elevated temperature dwell times. High-performance alloy test results for these thermal cycling profiles with the 10-minute well times were presented in six related papers between 2017 to 2022 [24-29].

The dwell time in the temperature cycling profile was an essential variable in the Alloy Alternatives Project. The dwell time segment of that expansive test plan included thirteen different SAC alloys, four temperature cycling profiles each with 10-minute and 60-minute dwell times, and two ball grid array (BGA) components, a 192-pin chip array BGA (192CABGA) and an 84-pin thin core BGA (84CTBGA) [2]. The bar charts in Figure 1 and Appendix A show the dwell time comparison for the four profiles, two BGA components and four SAC alloys. The per cent reduction in reliability (indicated by characteristic lifetime) resulting from the 60-minute dwell time varied widely with alloy composition, cycling profile, and component type and was described in detail in a previous publication [12]. The fracture characteristics and failure mode were found to be typical of SAC alloy thermal fatigue for all combinations of dwell time, temperature cycling profile, alloy, and component. In summary, the investigation demonstrated clearly that the longer thermal cycling dwell time reduced the characteristic lifetime over a range of 12-50% without altering the basic thermal fatigue failure mode in the bulk solder.

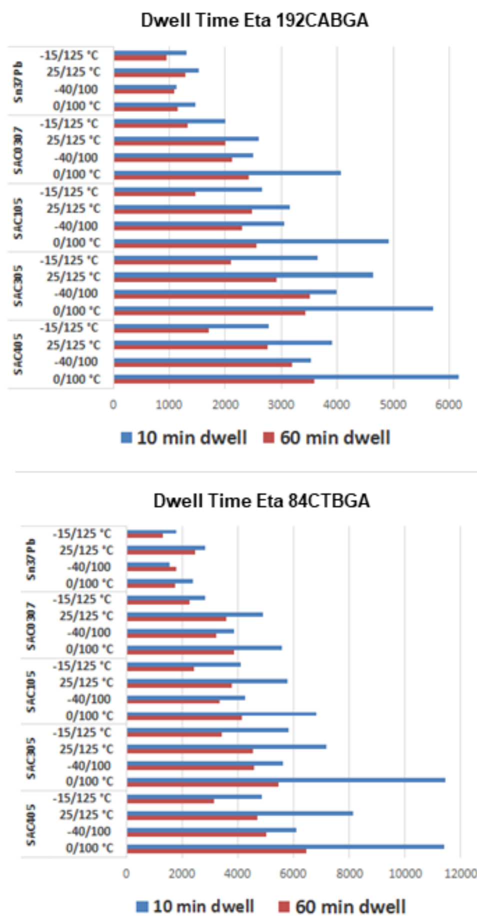

Figure 1. Bar charts illustrating the reduction in reliability with 60-minute dwell times from the alloy Alternatives project [12].

The dwell time effect has been reported and confirmed for different SAC solders alloys and a variety of area array, discrete, and quad flat no-lead (QFN) components [30-45]. The decrease in reliability under extended dwells is attributed to the longer stress relaxation duration of Pb-free solders compared to the former electronics industry de facto standard, eutectic SnPb solder. Extending the dwell time allows more creep deformation and increases the strain range [30, 40, 45], manifesting as a reduction in the number of cycles to failure.

Since the compositions of high-performance solder alloys are based on the SAC system, an extended dwell time is expected to have some bearing on board level attachment reliability [3, 22]. Any further dwell time effect related to the additional alloying elements, their strengthening mechanisms, and influence on microstructural evolution remains to be determined. This paper describes the planning and progress of the experimental program designed to assess the effect of a 60-minute temperature cycling dwell time on the thermal fatigue performance and microstructure of third generation, high-performance Pb-free solder alloys.

HIGH-PERFORMANCE Pb-FREE SOLDER ALLOYS

Background: Alloy Development and Requirements

The Sn-based, SAC alloys are more resistant to thermal fatigue than the eutectic SnPb alloy, but they have reliability limitations at higher operating temperatures [21]. During solidification of SAC solders, the Ag and Sn react to form networks of Ag_3Sn precipitates at the primary Sn dendrite boundaries. These intermetallic precipitates are recognized as the primary strengthening mechanism in SAC solders [23, 24, 32, 33]. During thermal or power cycling and extended elevated temperature exposure, the Ag_3Sn precipitates coarsen and become less effective in inhibiting dislocation movement and slowing damage accumulation. This pattern of microstructural evolution is characteristic of the thermal fatigue failure process in these Sn-based Pb-free alloys and was described originally in detail by Dunford et al in 2004 [46]. Figure 2 shows scanning electron micrographs illustrating coarsening of the Ag_3Sn precipitates in SAC305 solder caused by thermal cycling.

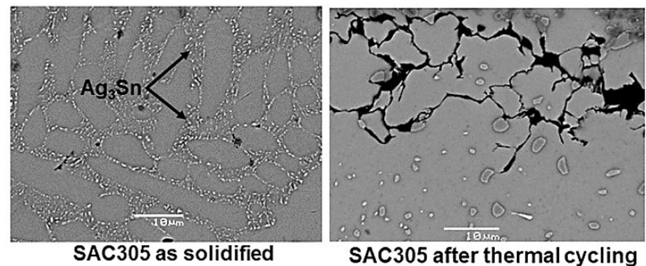

Figure 2. Backscattered scanning electron micrographs illustrating Ag3Sn intermetallic precipitate coarsening that precedes recrystallization and crack propagation during thermal cycling of SAC305.

The commercial motivation for development of third generation Pb-free high-performance is the dramatic increase

in electronic content in automobiles as illustrated in Figure 3 and Appendix B [47].

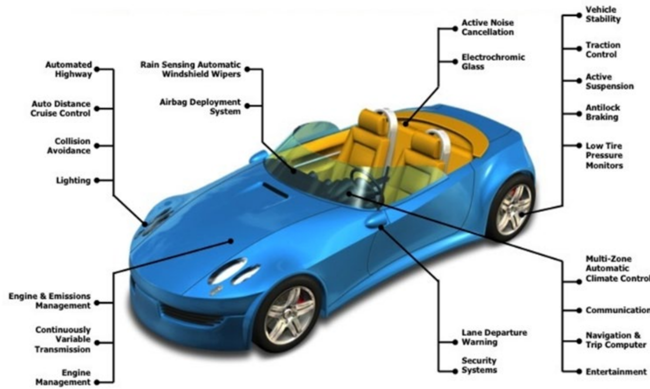

Figure 3. The proliferation of automotive sensors and electronic control modules [47].

Automotive electronic assemblies must perform in environments characterized by long dwell times at increasing temperatures, thermal and power cycling, vibration, and thermal and mechanical shock [22]. There is a concern that SAC alloys cannot satisfy the reliability requirements for these use environments. Automotive electronics no longer can be characterized simply as "under the hood." Figures 4a and 4b (and Appendix C) illustrate locations of sensors and control modules and the anticipated range of aggressive thermal exposures [48, 49]. Software and electronics design are now considered core competencies of automotive manufacturing, and this is driving innovation and an increase in electronic content for automotive applications.

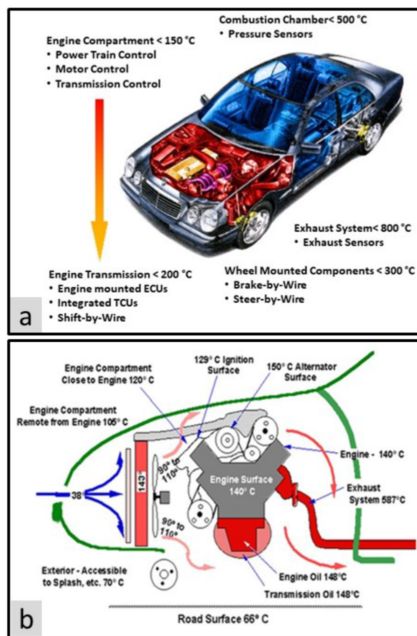

Figure 4. Illustrations of a) electronic control modules, sensor locations, and anticipated thermal exposures [48] and b) an engine compartment thermal profile [49].

The demand for solder alloys with better higher temperature performance has spawned the development of multiple commercial, high-performance Pb-free solder alloys. These alloys are based on the SAC system but have significant major and micro alloy additions to promote better elevated temperature performance. An additional goal is to increase resistance to damage from high strain rate mechanical loading, while maintaining superior resistance to thermal fatigue damage.

Early in the 21st century, when it appeared certain that the European Union RoHS Directive would proceed to implementation, a task group was formed of forward-looking solder suppliers, end users, and academic researchers with the objective to develop a commercial Pb-free alloy to meet the performance challenges of higher temperature automotive applications. The output of that working group was the initial third generation, commercial Pb-free solder alloy identified as Innolot or 90iSC [50-55]. The Innolot alloy is based on the ternary SAC387 formulation but contains significant alloying additions of bismuth (Bi) and antimony (Sb), along with a microalloy addition of nickel (Ni).

As the electronics industry considered the adoption of high-performance Pb-free solder alloys, the question of dwell time effect surfaced as it did with the adoption of SAC solder alloys. The addition of three element alloy additions, bismuth (Bi), antimony (Sb) and indium (In), are expected to make the dwell time and long-term metallurgical effects more complex and more critical to understand in terms of thermal solder fatigue and alloy performance.

The nominal compositions and melting ranges for the high-performance alloys included in this investigation are shown in Table 1. The test matrix contains the SAC305 alloy as the performance baseline. These alloys were down selected from the original, larger test matrix [22] based on prior alloy performance and resource considerations. Bismuth is the most common alloying element, which is confirmed by the attention given to Bi in the Pb-free alloy literature [21, 56-63]. Several SAC-based alloys contain a combination of Bi and Sb, and those alloys performed well in thermal cycling when tested with conventional, shorter dwell times [24-26]. Appendix D Metallurgical Considerations contains a review of the metallurgical basis for the alloying impact of Bi, Sb and In in Sn and SAC solders.

Table 1. The high-performance Pb-free solder alloys used to evaluate the effect of temperature cycling dwell time on thermal fatigue life and failure mode.

Alloy	Nominal Composition (wt. %)							Melting Range, °C
	Sn	Ag	Cu	Bi	Sb	In	other	
SAC305	96.5	3.0	0.5					217-221
Innolot	91.3	3.5	0.7	3.0	1.5		0.12 Ni	206-218
MaxRel Plus	91.9	4.0	0.6	3.5				212-220
M794	89.7	3.4	0.7	3.2	3.0		Ni	210-221
SB6NX	89.2	3.5	0.8	0.5		6.0		202-206
Violet	91.25	2.25	0.5	6.0				205-215
Indalloy 279	89.3	3.8	0.9		5.5	0.5		221-228
Indalloy 292	86.7	3.2	0.7	3,2	5.5	0.5		214-229
LF-C2	92.5	3.5	1.0	3.0				208-213

HIGH-PERFORMANCE Pb-FREE SOLDER ALLOYS

Background: Previous Performance in Thermal Cycling

The collaborative consortia project used the three thermal cycling profiles described in the INTRODUCTION, 0/100 °C, -40/125 °C, and -55/125 °C, with standard 10-to-15-minute dwell times, to evaluate the resistance to thermal cycling damage of multiple high-performance Pb-free solder alloys. Table 2 shows the complete list of alloys from that phase of the project. The alloys under evaluation with the 60-minute dwell times (Table 1) were down selected from this larger alloy matrix. The SAC305 hypoeutectic alloy is the performance baseline.

Table 2. The nominal compositions and melting ranges from the high-performance solder alloy investigation.

Alloy	Nominal Composition (wt. %)							Melting Range, °C
	Sn	Ag	Cu	Bi	Sb	In	other	
SAC305	96.5	3.0	0.5					217-221
Innolot	91.3	3.5	0.7	3.0	1.5		0.12 Ni	206-218
HT	95.0	2.5	0.5			2.0	Nd	206-218
MaxRel Plus	91.9	4.0	0.6	3.5				212-220
M794	89.7	3.4	0.7	3.2	3.0		Ni	210-221
M758	93.2	3.0	0.8	3.0			Ni	205-215
SB6NX	89.2	3.5	0.8	0.5		6.0		202-206
Violet	91.25	2.25	0.5	6.0				205-215
Indalloy 272	90.0	3.8	1.2	1.5	3.5			216-226
Indalloy 277	89.0	3.8	0.7	0.5	3.5	2.5		214-223
Indalloy 279	89.3	3.8	0.9		5.5	0.5		221-228
LF-C2	92.5	3.5	1.0	3.0				208-213
SN100CV	97.8		0.7	1.5			0.05Ni	221-225
405Y	95.5	4.0	0.5				0.05 Ni; Zn	217-221

The large volume of test data precluded simultaneous comparisons of all the alloys with the three temperature cycles and both components. Data targeting several pertinent alloy comparisons were released in four publications [25-28]. Some key results are summarized in the bar charts in Figure 5 (Appendix E) and Table 3 [25].

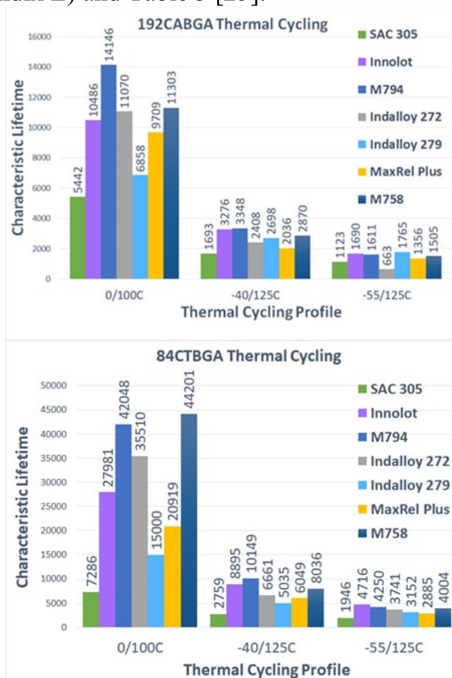

Figure 5. Bar charts comparing the characteristic lifetimes for the 192CABGA and 84CTBGA with SAC305 and the five high-performance solder alloys tested with the 0/100 °C, -40/125 °C and -55/125 °C thermal cycling profiles.

Table 3. Thermal cycling Weibull statistics for the alloys shown in Figure 5.

192CABGA Thermal Cycling Data				
Alloy	Temperature Cycle	Characteristic Lifetime h	Slope β	Correlation Coefficient, r^2
SAC305 (Sn3Ag0.5Cu)	0/100 °C	5442	6.6	0.95
	-40/125 °C	1693	3.6	0.99
	-55/125 °C	1123	6.1	0.98
Innolot (Sn3.5Ag0.7Cu3.0Bi1.5Sb0.12Ni)	0/100 °C	10486	6.7	0.93
	-40/125 °C	3276	7.0	0.98
	-55/125 °C	1690	2.6	0.97
M794 (Sn3.4Ag0.7Cu3.3Bi3.0Sb)	0/100 °C	14146	3.8	0.97
	-40/125 °C	3348	8.2	0.97
	-55/125 °C	1611	4.6	0.98
Indalloy 272 (Sn3.8Ag1.2Cu1.5Bi3.5Sb)	0/100 °C	11070	4.6	0.95
	-40/125 °C	2408	4.3	0.96
	-55/125 °C	663	1.9	0.92
Indalloy 279 (Sn3.8Ag0.9Cu5.5Sb0.5In)	0/100 °C	6858	7.0	0.97
	-40/125 °C	2698	7.4	0.96
	-55/125 °C	1765	7.2	0.96
MaxRel Plus (Sn4.0Ag0.6Cu3.5Bi)	0/100 °C	9709	4.0	0.96
	-40/125 °C	2036	8.0	0.94
	-55/125 °C	1356	5.7	0.93
M758 (Sn3.0Ag0.8Cu3.0Bi)	0/100 °C	11303	3.0	0.94
	-40/125 °C	2870	5.7	0.89
	-55/125 °C	1505	3.4	0.96
84CTBGA Thermal Cycling Data				
Alloy	Temperature Cycle	Characteristic Lifetime h	Slope β	Correlation Coefficient r^2
SAC305 (Sn3Ag0.5Cu)	0/100 °C	7287	8.3	0.98
	-40/125 °C	2759	9.5	0.94
	-55/125 °C	1946	8.3	0.99
Innolot (Sn3.5Ag0.7Cu3.0Bi1.5Sb0.12Ni)	0/100 °C	27981	4.5	0.94
	-40/125 °C	8895	8.8	0.88
	-55/125 °C	4716	5.5	0.98
M794 (Sn3.4Ag0.7Cu3.3Bi3.0Sb)	0/100 °C	42048	6.2	0.88
	-40/125 °C	10149	4.6	0.94
	-55/125 °C	4250	2.3	0.91
Indalloy 272 (Sn3.8Ag1.2Cu3.5Sb1.5Bi)	0/100 °C	35510	6.8	0.95
	-40/125 °C	6661	7.2	0.96
	-55/125 °C	3741	4.6	0.99
Indalloy 279 (Sn3.8Ag0.9Cu5.5Sb0.5In)	0/100 °C	15000	5.9	0.94
	-40/125 °C	5035	9.8	0.97
	-55/125 °C	3152	6.3	0.99
MaxRel Plus (Sn4.0Ag0.6Cu3.5Bi)	0/100 °C	20919	4.3	0.97
	-40/125 °C	6049	5.4	0.98
	-55/125 °C	2885	7.9	0.95
M758 (Sn3.0Ag0.8Cu3.0Bi)	0/100 °C	44201	4.1	0.93
	-40/125 °C	8036	5.1	0.97
	-55/125 °C	4004	4.8	0.96

The high-performance alloys outperformed the SAC305 baseline with a single exception, the Indalloy 272 alloy with the 192CABGA component and -55/125 °C cycling. With the standard dwell time tests, thermal fatigue in the bulk solder was the prevailing though not exclusive failure mode for all combinations of alloys, thermal cycles, and components. However, interfacial, and mixed mode (thermal fatigue and interfacial cracking) failures were found in some 192CABGA samples with all the alloys. Interfacial cracking was more pronounced with the more aggressive -55/125 °C thermal cycling, and there appeared to be a correlation between interfacial cracking and a decrease in the characteristic lifetime and slope of Indalloy 272. The occurrence of interfacial and mixed mode cracking did not affect the Weibull statistics for the other alloys. No interfacial cracking was detected in SAC305 after testing, and there was no evidence of interfacial cracking prior to testing in any of the samples.

The data for the 84CTBGA are better-behaved than the 192CABGA and show greater separation between highest and lowest performers. This observation is consistent with the results for the other alloys in the study [26-28]. Compared to the 192CABGA, the 84CTBGA did not demonstrate the

same susceptibility to the interfacial failure mode. Because it is less susceptible to interfacial cracking than the 192CABGA, the 84CTBGA appears to better component for measuring fatigue performance. Indalloy 272 for example, performs poorly with the 192CABGA but performs closer to expectations with the 84CTBGA. Figure 6 (Appendix F) compares failure modes for the 192CABGA and 84CTBGA.

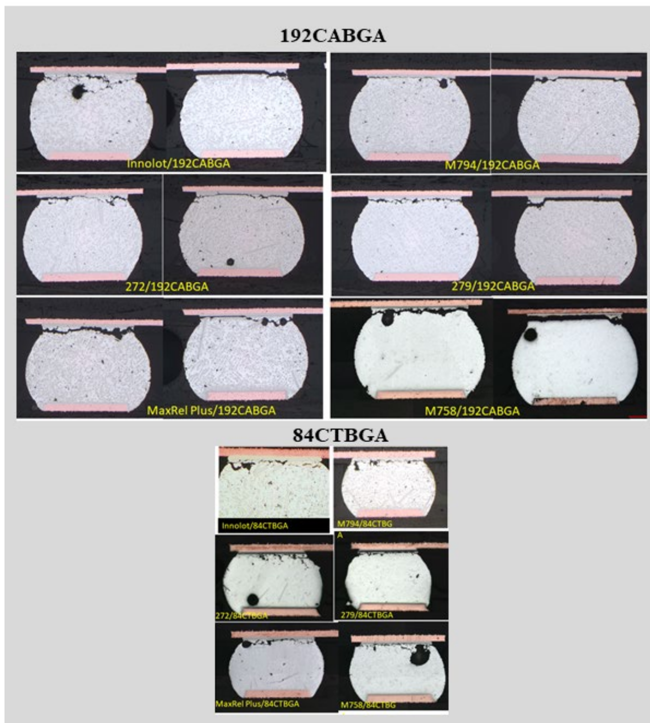

Figure 6. Optical photomicrographs showing examples of thermal fatigue damage and interfacial fracturing in the solder joints of the 192CABGA for all the high-performance solder alloys (upper), and solder fatigue damage only in the solder joints of the 84CTBGA for all high-performance alloys. SAC305 exhibits only fatigue damage with both components. The thermal cycling test profile was -55/125 °C (TC4).

These results indicated combinations of Bi and Sb were more effective than either element as a single alloying addition, although the reliability margins in thermal cycling tests were not always great or statistically significant. Regardless of the limitations quantifying reliability performance, all the high-performance alloys outperform SAC305 consistently and by significant margins. Furthermore, the emerging trend is that the best performing alloys contain a combination of Bi and Sb, particularly those that are most highly alloyed such as M794 and Innolot.

EXPERIMENTAL

Test Vehicle

Component and Test Board Description

This study utilizes the components and printed circuit board (PCB) developed as the test vehicle for the iNEMI Alloy Alternatives study [2]. The two daisy-chained ball grid arrays (BGA), a 192 I/O chip array BGA (192CABGA) and an 84 I/O thin core chip array (84CTBGA) are shown in Figure 7 and Appendix G [64]. The parts were purchased as land-grid arrays (LGA) to enable subsequent attachment of the various Pb-free-alloy spheres included in the scope of the program (Table 1).

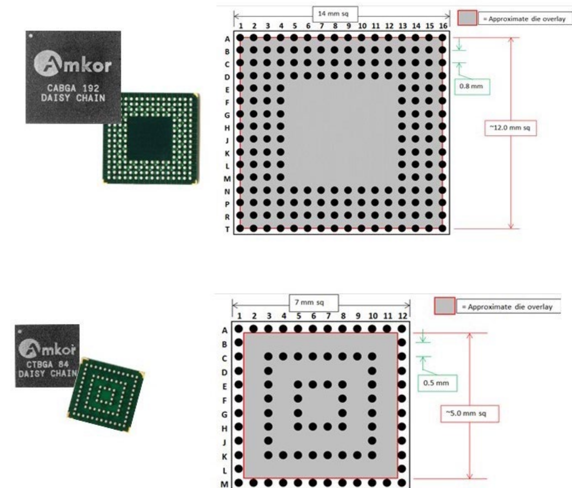

Figure 7. The 192CABGA and 84CTBGA daisy chained components and pin diagrams with die size and location [64].

The printed circuit board (PCB) test vehicle is 2.36 mm (93 mils) thick, with a 6-layer construction with 16 sites for the larger 192CABGA, and another 16 sites for the 84CTBGA (Figure 8 and Appendix G). The boards were fabricated with the Panasonic R-1755V high temperature laminate material and the final finish is a high temperature organic solderability preservative (OSP). The complete attributes of the components and PCB are contained in Table 4.

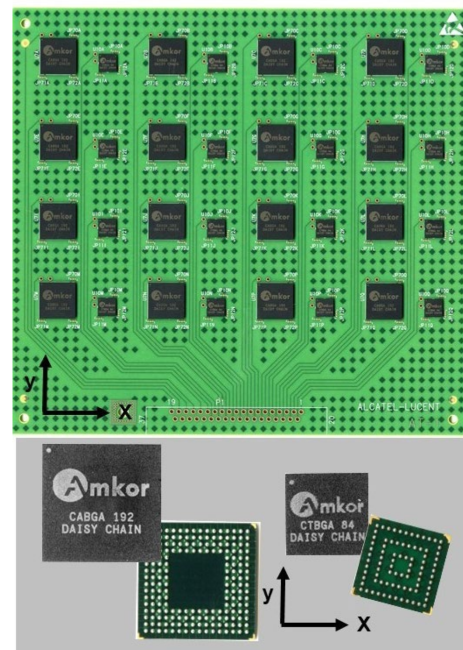

Figure 8. A fully populated, daisy chained Alloy Alternatives test vehicle.

Table 4. Ball grid array (BGA) and printed circuit board (PCB) test vehicle attributes.

BGA Package Attributes		
Designation	192CABGA	84CTBGA
Die Size	12x12 mm	5x5 mm
Package Size	14x14 mm	7x7 mm
Ball Array	16x16	12x12
Ball Pitch	0.8 mm	0.5 mm
Ball Diameter	0.46 mm	0.3 mm
Pad Diameter	0.381 mm	0.3 mm
Pad Finish	Electrolytic Ni/Au	Electrolytic Ni/Au
Au thickness	0.6 mm	0.6 mm
PCB Attributes		
Dimensions	165 x 178 x 2.36 mm	
Laminate	Panasonic R-1755V	
Surface Finish	Entek HT OSP	
No. Cu Layers	6	
Pad Diameter	0.356 mm	0.254 mm
Solder Mask Dia.	0.483 mm	0.381 mm
Laminate	Panasonic R-1755V	
Glass Transition Temperature, T_g	165 °C	
Decomposition Temperature, T_d	350 °C	
Room Temperature Storage Modulus	11.6 Gpa	

Solder joint attachment reliability is dependent strongly on the coefficient of thermal expansion (CTE) mismatch (difference) between the package and the PCB as well as the distance from neutral point (DNP) [65]. Although the small chip array package sizes used in this study minimize the DNP effect, their large die to package ratios (DPR) result in substantial CTE mismatch [65]. The modulus or stiffness of the PCB also can affect solder joint reliability.

The CTE of the PCB was measured using a thermomechanical analyzer (TMA) and the composite coefficients of thermal expansion of the BGA packages were measured using microscopic Moiré interferometry. The data in Table 5a show a lower composite CTE for the 192CABGA package. The lower CTE of the 192CABGA results in a larger CTE mismatch with the PCB, hence the thermal cycling lifetime of the 192CABGA is shorter than that of the 84CTBGA [25-28]. The CTE data for the PCB laminate material are shown in Table 5b.

Table 5a. CTE of the BGA component test vehicles measured by microscopic Moiré interferometry.

BGA Package	Effective CTE α (ppm/°C) T °C:24~130	
	x-direction	y-direction
192CABGA	8.6	10.1
84CTBGA	10.9	11.0

Table 5b. CTE of the Panasonic R-1755R laminate material measured with a thermomechanical analyzer (TMA).

Panasonic R-1755V	
Effective CTE α (ppm/°C) T °C:20~140	
x-direction	y-direction
13.5	16.1

Component Ball Attachment Process

The parts were purchased as land-grid arrays (LGA) to enable subsequent attachment of each of the different high-performance Pb-free-alloy balls included in the scope of the program (Table 1). The ball attachment was performed at SemiPack (https://www.semipack.com) using the same process developed for the iNEMI Alternative Alloys project [2].

Test Vehicle Surface Mount Assembly

The solder assembly of the test vehicles was performed at Collins Aerospace, Cedar Rapids, IA. A pilot build using SAC305 components and paste was conducted to establish the stencil printing and reflow process parameters. A 5-mil (125 µm) thick stencil was used with 14 mil (0.35 mm) diameter round apertures for the larger 192CABGA and 12 mil x 12 mil (0.3 mm x 0.3 mm) square apertures for the smaller 84CTBGA. The test vehicles were reflowed in a 14-temperature zone convection oven in a nitrogen atmosphere. Type 4 no-clean solder paste was used for all the final assemblies. The nominal peak temperature measured on the board adjacent to the solder joints was 245 °C.

Accelerated Temperature Cycling

Accelerated temperature cycling (ATC) is the recognized technique for evaluating the thermal fatigue performance of solder attachments. The daisy-chained components and the test circuit boards enabled electrical continuity testing after surface mount assembly and in situ, continuous monitoring during thermal cycling. Thermal cycling is done in accordance with the IPC-9701B guideline [23]. The solder joint resistance is monitored using either an event detector or a data logger set at a resistance limit of 1000 ohm, also described previously [2]. The failure data will be reported as characteristic life η (the number of cycles to achieve 63.2% failure), slope β, and cumulative 1% failure from a two-parameter Weibull analysis.

The nominal temperature cycling profiles for this investigation are shown in Table 6. These profiles are selected to address the requirements of three specific industries or market segments as defined in IPC-9701B with telecom represented by TC1, consumer/handheld by TC4, and military/defense by TC7. The 60-minute dwell times return only ten cycles per day, which results in exceedingly long test durations.

Each alloy test cell contains two fully populated replicate test boards to provide a sample size of 32 BGA components of each type for thermal cycling and an additional populated test

board for baseline quality and microstructural characterization.

Table 6. Temperature cycling profiles**.**

Thermal Cycle	Minimum Temp. (°C)	Maximum Temp. (°C)	Temp. Range ΔT (°C)	Dwell Time (min.)
TC1	0	100	100	60
TC4	-40	125	165	60
TC7	-55	125	180	60

Microstructural Characterization and Failure Analysis
Optical metallography (destructive cross-sectional analysis) and scanning electron microscopy (SEM) are used to document the solder joint quality and basic solder microstructures of representative board level assemblies from each of the component and alloy test cells. The baseline characterization before temperature cycling enables microstructural comparisons to samples selected for failure mode analysis after temperature cycling. The SEM operating in the backscattered electron imaging (BEI) mode is effective for differentiating phases in SAC microstructures [25-28], but more sophisticated methods are required to detect and quantify certain phases in the high-performance alloys [66, 67].

DISCUSSION
The test results from the Alloy Alternatives project confirmed the inverse relationship between thermal cycling dwell time and resistance to thermal fatigue using a series of SAC Pb-free alloys. In that series of tests, the failure mode consistently was by thermal fatigue in the bulk solder under all thermal cycling test conditions (profiles), but the percent reduction in reliability varied widely based on alloy Ag content and test profile. Because high-performance solder alloys are based on the SAC system, it seems likely that a longer dwell time would reduce the board level reliability of these alloys [3, 22]. Although some dwell effect is anticipated due to Ag_3Sn precipitate coarsening, dwell time effects related to the major alloying elements, indium (In), Antimony (Sb), and bismuth (Bi), and their strengthening mechanisms, and influence on microstructural evolution remain to be determined.

The effect of indium (In) on thermal cycling performance is evaluated in this study primarily with the alloy designated SB6NX. SB6NX is SAC-based with 3.5 wt. % Ag and 6 wt. % In (Table 2) and only a minor 0.5 wt. % addition of Bi. The optimized alloy composition of 6 wt. % In was based on thermal cycling trials by the alloy developer using a range of In content from 2-10%. That trial concluded reliability in thermal cycling was optimized with 6 wt.% In [68, 69]. The bar chart in Figure 9 and Appendix H shows the performance of SB6NX with 10-minute dwell times and the (better-behaved) 84CTBGA component to be better than SAC305, but not as good as the other high-performance alloys.

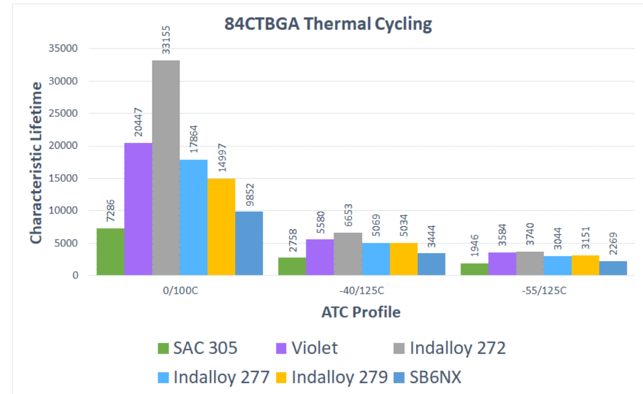

Figure 9. Bar charts comparing the characteristic lifetimes for the 84CTBGA with SAC305, and five high-performance solder alloys tested with the 0/100 °C, -40/125 °C and -55/125 °C thermal cycling profiles [26].

The enhanced performance of SB6NX is attributed to substitutional solid solution strengthening of In in Sn [3]. Indium also forms many intermetallic compounds (IMC) or intermediate phases with Sn, Au, Ag, Sb, and Cu, which do not enhance performance [66]. Extraneous phase formation depletes the amount of In in solid solution and may account for the relatively high In content needed to optimize performance. Extending the dwell time to 60-minutes could cause further IMC formation or growth of existing precipitates, thereby depleting the In from solution, and making the alloy more susceptible to failure. This would manifest as a greater per cent reduction in reliability than expected and drive the performance of SB6NX even closer to SAC305.

The enhanced performance of Indalloy 279 is attributed primarily to precipitation strengthening from the SbSn intermetallic compound [3], although there may be a minor contribution from substitutional solid solution strengthening of Sb in Sn. The SbSn phase precipitates inside β-Sn dendrites providing strengthening particles in the dendritic β-Sn to supplement strengthening from the Ag_3Sn particles in the eutectic regions. The SbSn precipitates are smaller than the Ag_3Sn, but they coarsen rapidly, similarly to the Ag_3Sn with enhanced particle coarsening in the region of localized shear strain and recrystallisation near the component side [70]. Extending the dwell time to 60-minutes could diminish the effectiveness of the SbSn particles, but the performance of Indalloy 279 should still be superior to SAC305.

The enhanced performance of alloys such as MaxRel Plus, M758, and Violet is attributed to solid solution or dispersion strengthening of Bi in Sn [3]. Fundamental studies leave no doubt that Bi additions can have a positive effect on the physical properties of Sn-based solder alloys [57, 58, 61, 71, 72]. Results from the 10-mnute dwell thermal cycling studies, however, are not clear-cut [25-27]. There are differences in Ag content among these alloys (Table 2), which is important

because the formation of Ag_3Sn precipitates is still the primary strengthening agent. There also are significant variations in Weibull slope (β) across the data sets (Table 3) and these β variations limit quantitative comparisons. These β variations, at least in the case of the 192CABGA, have been linked to the interfacial (non-fatigue) failure mode, which complicates comparisons further (Figure 6).

It is difficult to anticipate the effect of the extended, 60-minute dwell time on the performance of alloys that employ Bi as their primary strengthening agent. The solubility of Bi in Sn is approximately 1.5 wt. % at room temperature, but typically high-performance alloys contain enough Bi to take advantage of the Bi solubility limit at higher temperatures. The Bi distribution and microstructure depend on solidification conditions and subsequent thermal exposure, which determine the relative contributions of Bi to solid solution and dispersion strengthening [68]. After repeated, extended dwell exposures at the upper temperature extreme, it is not known if the Bi will continue to be effective by remaining in solution or by precipitating as a dispersoid. Because Bi does not always precipitate homogeneously, it is possible that adding enough Bi to take advantage of the Bi solubility limit at higher temperatures may have a diminishing or negative effect on reliability. The outcomes also could vary significantly with thermal cycling profile and upper temperature extreme (Table 6).

The results from the 10-minute dwell time testing indicated combinations of Bi and Sb were more effective than either element as a single alloying addition, although the reliability margins in thermal cycling tests were not always great or statistically significant. The emerging trend based on the 10-minute dwell testing is that the best performing alloys contain a combination of Bi and Sb, particularly those that are most highly alloyed such as M794 and Innolot. Even with their excellent performance, these alloys often did not fail exclusively by solder fatigue in the earlier, 10-minute dwell tests (Figure 6). This interfacial cracking is perplexing because in thermal cycling typically it typically manifests as an early life, catastrophic failure, and there was no convincing evidence of that in the Weibull plots for any of the best-performing alloys. Because the root cause of interfacial cracking was not resolved in the earlier study, it is difficult to predict the outcome when the dwell time is extended to 60 minutes.

The impact of the aggressive -55/125 ºC test condition is another factor to be considered. This test condition was not used in the Alloy Alternatives project but was inserted into the current study to address alloy performance in more aggressive use environments by using a higher upper temperature extreme and greater strain (ΔT). With the 10-minute dwell time and -55/125 ºC test condition, the reliability margins were not great as shown in the bar charts of Figure 5. The results also are not always statistically significant [25]. It will be interesting to see if this trend continues with the 60-minute dwell times or if the longer dwell induces more separation in alloy performance. If more separation is observed, this would provide better insight into alloy performance in the most challenging applications that are the target for high-performance alloy development.

STATUS AND NEXT STEPS

As detailed in the DISCUSSION and Appendix D, the addition of constituent elements (Bi, Sb, In) to SAC-type solder alloys is specifically aimed at improving solder alloy reliability through microstructural development and microstructural evolution. Depending on the constituent element additions, solder alloy properties such as resistance to fatigue and creep are improved by substitutional solid solution hardening, precipitation hardening, and dispersoid hardening. The utilization of these metallurgical strengthening mechanisms is a new direction for the electronics industry in terms of solder alloy design but is a widespread practice in many other metal alloy systems. For example, aluminum alloys 2024 and 7075 that are used widely in aircraft applications, have significantly improved mechanical properties due to the addition of copper and zinc, respectively [73, 74]. These aluminum alloys are solution heat treated allowing for the copper or zinc to be distributed within the aluminum alloy crystal structure and then quenched, fixing their positions in the crystal structure. A subsequent detailed heat treatment process is conducted forming precipitates that inhibit dislocation movement and slow damage accumulation.

The current experimental program is designed to assess the effect of a 60-minute temperature cycling dwell time on the thermal fatigue performance and microstructure of high-performance Pb-free solder alloys that use these same metallurgical principles for alloy strengthening. Microstructural and failure mode analyses will be conducted upon the completion of the thermal cycle testing to understand how the Bi, Sb and In constituent element additions modify the solder alloys and respond to the extended dwell time during thermal cycling. At the time of this writing, the three temperature cycling tests were running but there was insufficient progress to enable meaningful data reporting and sample removal for failure analysis. The success or failure of applying the metallurgical principles to these high-performance Pb-free solder alloys will be reported in future publications.

ACKNOWLEDGEMENTS

The authors thank the staffs at iNEMI and the HDP User Group, especially Grace O'Malley, Shekhar Chandrashekhar, and Larry Marcanti for their help in establishing and nurturing the collaborative agreement and for their continued support in coordinating the work between the cooperating consortia. Many thanks to Jim Fuller of Sanmina for PCB test vehicle support. The authors also express gratitude to their respective companies that have supported the various phases

of the iNEMI Alloy Project to evaluate alternative Pb-free solder alloys for over a decade including the current collaborative Phase 4 program between iNEMI and HDP that is exploring high-performance Pb-free solder alloys.

REFERENCES

1] "Annex to Directive 2002/95/EC, Restriction on the use of hazardous substances (RoHS) in electrical and electronic equipment," *Official Journal of the European Union*, 14.10.2006, L283/48-49, October 12, 2006.

[2] Gregory Henshall, Jian Miremadi, Richard Parker, Richard Coyle, Joe Smetana, Jennifer Nguyen, Weiping Liu, Keith Sweatman, Keith Howell, Ranjit S. Pandher, Derek Daily, Mark Currie, Tae-Kyu Lee, Julie Silk, Bill Jones, Stephen Tisdale, Fay Hua, Michael Osterman, Bill Barthel, Thilo Sack, Polina Snugovsky, Ahmer Syed, Aileen Allen, Joelle Arnold, Donald Moore, Graver Chang, and Elizabeth Benedetto, "iNEMI Pb-Free Alloy Characterization Project Report: Part I – Program Goals, Experimental Structure, Alloy Characterization, and Test Protocols for Accelerated Temperature Cycling," *Proceedings of SMTAI 2012*, 335-347, Orlando, FL, October, 2012.

[3] Richard J. Coyle, "Chapter 7: Lead (Pb)-Free Solders for High Reliability and High-Performance Applications," in Lead-free Soldering Process Development and Reliability, Jasbir Bath, editor, 191-248, John Wiley & Sons, Inc. Print July 28, 2020, ISBN 9781119482031, online July 3, 2020, ISBN 9781119482093.

[4] Gregory Henshall, Keith Sweatman, Keith Howell, Joe Smetana Richard Coyle, Richard Parker, Stephen Tisdale, Fay Hua, Weiping Liu, Robert Healey, Ranjit S. Pandher, Derek Daily, Mark Currie, and Jennifer Nguyen, "iNEMI Lead-Free Alloy Alternatives Project Report: Thermal Fatigue Experiments and Alloy Test Requirements," *Proceedings of SMTAI*, 317-324, San Diego CA, 2009.

[5] Joe Smetana, Richard Coyle, Peter Read, Richard Popowich, Debra Fleming, and Thilo Sack, "Variations in Thermal Cycling Response of Pb-free Solder Due to Isothermal Preconditioning," *Proceedings of SMTAI 2011*, 641-654, Fort Worth, TX, October 2011.

[6] Werner Engelmaier, "Surface Mount Solder Joint Long-Term Reliability: Design, Testing, Prediction," *Soldering and Surface Mount Technology*, vol. 1, no. 1, 14-22, February 1989.

[7] Richard Coyle, Keith Sweatman, and Babak Arfaei, "Thermal Fatigue Evaluation of Pb-Free Solder Joints: Results, Lessons Learned, and Future Trends," *JOM*, Vol. 67, No. 10, 2015.

[6] Richard Coyle, Richard Parker, Joseph Smetana, Elizabeth Benedetto, Keith Howell, Keith Sweatman, Weiping Liu, Michael Osterman, Julie Silk, Aileen Allen, Mitch Holtzer, Rafael Padilla, and Tomoyasu Yoshikawa "iNEMI Pb-Free Alloy Characterization Project Report: PART IX – Summary of the Effect of Isothermal Preconditioning on Thermal Fatigue Life," *Proceedings of SMTAI 2015*, 743-755, Chicago, IL, September 27 –October 1, 2015.

[9] Richard Coyle, Richard Parker, Elizabeth Benedetto, Keith Howell, Keith Sweatman, Stuart Longgood, Joseph Smetana, Aileen Allen, Peter Read, Babak Arfaei, and Francis Mutuku, "iNEMI Pb-Free Alloy Characterization Project Report: PART VIII - Thermal Fatigue Results for High-Ag Alloys at Extended Dwell Times," *Proceedings of SMTAI 2014*, 547-560, Chicago, IL, October 2014.

[10] Keith Sweatman, Richard Coyle, Richard Parker, Keith Howell, Elizabeth Benedetto, Joseph Smetana, Aileen Allen, Weiping Lui, Julie Silk, "iNEMI Pb-Free Alloy Characterization Project Report: PART VII - Thermal Fatigue Results for Low-Ag Alloys at Extended Dwell Times," *Proceedings of SMTAI 2014*, 561-574, Chicago, IL, October 2014.

[11] Richard Coyle, Richard Parker, Babak Arfaei, Francis Mutuku, Keith Sweatman, Keith Howell, Stuart Longgood, and Elizabeth Benedetto, The Effect of Nickel Microalloying on Thermal Fatigue Reliability and Microstructure of SAC105 and SAC205 Solders, *Proceedings of Electronic Components Technology Conference*, 425-440, IEEE, Orlando, FL, 2014.

[12] Richard Coyle, Richard Parker, Michael Osterman, Stuart Longgood, Keith Sweatman, Elizabeth Benedetto, Aileen Allen, Elviz George, Joseph Smetana, Keith Howell, and Joelle Arnold, "iNEMI Pb-Free Alloy Characterization Project Report: Part V – The Effect of Dwell Time on Thermal Fatigue Reliability," *Proceedings of SMTAI 2013*, 470-489, Ft. Worth, TX, October 2013.

[13] Richard Coyle, Richard Parker, Babak Arfaei, Keith Sweatman, Keith Howell, Stuart Longgood, and Elizabeth Benedetto, "iNEMI Pb-Free Alloy Characterization Project Report: Part VI – The Effect of Component Surface Finish and Solder Paste Composition on Thermal Fatigue of SN100C Solder Balls," *Proceedings of SMTAI 2013*, 490-414, Ft. Worth, TX, October 2013.

[14] Elviz George, Michael Osterman, Michael Pecht, Richard Coyle, Richard Parker, and Elizabeth Benedetto, "Thermal Cycling Reliability of Alternative Low-Silver Tin-based Solders," *Proceedings of IMAPS 2013, 46th International Symposium on Microelectronics*, Orlando, FL, October 2013.

[15] Richard Parker, Richard Coyle, Gregory Henshall, Joe Smetana, and Elizabeth Benedetto, "iNEMI Pb-Free Alloy Ch5racterization Project Report: Part II – Thermal Fatigue Results for Two Common Temperature Cycles," *Proceedings of SMTAI 2012*, 348-358, Orlando, FL, October 2012.

[16] Keith Sweatman, Keith Howell, Richard Coyle, Richard Parker, Gregory Henshall, Joe Smetana, Elizabeth Benedetto, Weiping Liu, Ranjit S. Pandher, Derek Daily, Mark Currie, Jennifer Nguyen, Tae-Kyu Lee, Michael Osterman, Jian Miremadi, Aileen Allen, Joelle Arnold, Donald Moore, Graver Chang, "iNEMI Pb-Free Alloy Characterization Project Report: Part III - iNemi Pb-Free Alloy Characterization Project Report: Part III - Thermal Fatigue Results For Low-Ag Alloys," *Proceedings of SMTAI 2012,* 359-375, Orlando, FL, October 2012.

[17] Richard Coyle, Richard Parker, Gregory Henshall, Michael Osterman, Joe Smetana, Elizabeth Benedetto, Donald Moore, Graver Chang, Joelle Arnold, and Tae-Kyu Lee, "iNEMI Pb-Free Alloy Characterization Project Report:

Part IV - Effect of Isothermal Preconditioning on Thermal Fatigue Life," *Proceedings of SMTAI 2012*, 376-389, Orlando, FL, October 2012.

[18] Gregory Henshall, Robert Healey, Ranjit S. Pandher, Keith Sweatman, Keith Howell, Richard Coyle, Thilo Sack, Polina Sngovsky, Stephen Tisdale and Fay Hua, and Grace O'Malley, "Addressing the opportunities and risks of pb-free solder alloy alternatives," *Proceedings of Microelectronics and Packaging Conference 2009*, EMPC European 2009, 1-11, Rimini, Italy, June 2009.

[19] Gregory Henshall, Robert Healy, Ranjit S. Pander, Keith Sweatman, Keith Howell, Richard Coyle, Thilo Sack, Polina Snugovsky, Stephen Tisdale, and Fay Hua, "iNEMI Pb-free Alloy Alternatives Project Report: State of the Industry, *SMT Journal*, Volume 21, Issue 4, 11-23, October-December 2008.

[20] Gregory Henshall, Robert Healy, Ranjit S. Pander, Keith Sweatman, Keith Howell, Richard Coyle, Thilo Sack, Polina Snugovsky, Stephen Tisdale, and Fay Hua, "iNEMI Pb-free Alloy Alternatives Project Report: State of the Industry, *Proceedings of SMTAI 2008*, 109-122, Orlando, FL, August 2008.

[21] Polina Snugovsky, Simin Bagheri, Marianne Romansky, Doug Perovic, Leonid Snugovsky, and John Rutter, "New Generation Of Pb-Free Solder Alloys: Possible Solution To Solve Current Issues With Main Stream Pb-Free Soldering," SMTA J., **Vol. 25**, issue 3, 42-52, July 2012.

[22] Richard Coyle, Richard Parker, Keith Howell, Dave Hillman, Joe Smetana, Glen Thomas, Stuart Longgood, Michael Osterman, Eric Lundeen, Polina Snugovsky, Julie Silk, Andre Kleyner, Keith Sweatman, Rafael Padilla, Tomoyasu Yoshikawa, Jasbir Bath, Mitch Holtzer, Hongwen Zhang, Jerome Noiray, Frederic Duondel, Raiyo Aspandiar, and Jim Wilcox, "A Collaborative Industrial Consortia Program for Characterizing Thermal Fatigue Reliability of Third-Generation Pb-Free Alloys," *Proceedings of SMTAI 2016*, 188-196, Rosemont, IL, September 2016.

[23] IPC-9701B, "Thermal Cycling Test Method for Fatigue Life Characterization of Surface Mount Attachments," IPC, Bannockburn, IL, 2021.

[24] Tim Pearson, Richard Coyle, Michael Osterman, Faramarz Hadian, Dave Hillman, Charmaine Johnson, Jeffrey Chumbley, Xinzhi Feng, Joe Smetana, Keith Howell, Julie Silk, Babak Arfaei, Hongwen Zhang, Jie Geng, Derek Daily, Ranjit Pandher, Shantanu Joshi, Stuart Longgood, and Andre Kleyner, "Thermal Fatigue Reliability of a 1206 Chip Resistor with High-Performance Pb-Free Solder Alloys," *Proceedings of SMTAI International*, Minneapolis, MN, October 31- November 3, 2022.

[25] Richard Coyle, Charmaine Johnson, Dave Hillman, Tim Pearson, Michael Osterman, Joe Smetana, Keith Howell, Hongwen Zhang, Julie Silk, Jie Geng, Derek Daily, Babak Arfaei, Ranjit Pandher, Andre Delhaise, Stuart Longgood, and Andre Kleyner, "Enhancing Thermal Fatigue Reliability of Pb-Free Solder Alloys with Additions of Bismuth and Antimony," *Proceedings of SMTAI 2020 Virtual*, 339-354, September 28 - October 23, 2020.

[26] Richard Coyle, Charmaine Johnson, Dave Hillman, Richard Parker, Michael Osterman, Joe Smetana, Tim Pearson, Babak Arfaei, Keith Howell, Stuart Longgood, Andre Kleyner, Julie Silk, Andre Delhaise, Hongwen Zhang, Jie Geng, Ranjit Pandher, and Eric Lundeen, "Thermal Cycling Reliability and Failure Mode of Two Ball Grid Array packages with High Reliability Pb-Free Solder Alloys," *Proceedings of SMTAI*, 439-456, Rosemont, IL, September 2019.

[27] Richard Coyle, Dave Hillman, Richard Parker, Charmaine Johnson, Michael Osterman, Jasbir Bath, Babak Arfaei, Andre Delhaise, Keith Howell, Brook Sandy-Smith, Joe Smetana, Stuart Longgood, "The Effect of Bismuth, Antimony, or Indium on the Thermal Fatigue of High Reliability Pb-Free Solder Alloys," *Proceedings of SMTAI*, Rosemont, IL, October 2018.

[28] Richard Coyle, Dave Hillman, Charmaine Johnson, Richard Parker, Brook Sandy-Smith, Hongwen Zhang, Jie Geng, Michael Osterman, Babak Arfaei, Andre Delhaise, Keith Howell, Jasbir Bath, Joe Smetana, Stuart Longgood, Andre Kleyner, Julie Silk, Ranjit Pandher, Eric Lundeen, and Jerome Noiray "Alloy Composition and Thermal Fatigue of High Reliability Pb-Free Solder Alloys," *Proceedings of SMTAI*, Rosemont, IL, October 2018.

[29] Richard Coyle, Raiyo Aspandiar, Michael Osterman, Charmaine Johnson, Richard Popowich, Richard Parker, Dave Hillman, "Thermal Cycle reliability of a Low Ag Ball Grid Array Assembled with Tin Bismuth Solder paste," *Proceedings of SMTAI*, 108-116, Rosemont, IL, September 17-21, 2017.

[30] Elviz George, Michael Osterman, Michael Pecht, and Richard Coyle, "Effects of Extended Dwell Time on Thermal Fatigue Life of Ceramic Chip Resistors," *Proceedings of IMAPS 2012 45th International Symposium on Microelectronics*, San Diego, CA, September 2012.

[31] Richard Coyle, Peter Read, Heather McCormick, Richard Popowich, and Debra Fleming, "The Influence of Alloy Composition and Temperature Cycling Dwell Time on the Reliability of a Quad Flat No Lead (QFN) Package," *Journal of SMT*, Vol. 25, Issue 1, 28-34, January-March 2011.

[32] Richard Coyle, John Osenbach, Maurice Collins, Heather McCormick, Peter Read, Debra Fleming, Richard Popowich, Jeff Punch, Michael Reid, and Steven Kummerl, "Phenomenological Study of the Effect of Microstructural Evolution on the Thermal Fatigue Resistance of Pb-Free Solder Joints," *IEEE Trans. CPMT*, Vol. 1, No. 10, 1583-1593, October 2011.

[33] Richard Coyle, Heather McCormick, John Osenbach, Peter Read, Richard Popowich, Debra Fleming, and John Manock, "Pb-free Alloy Silver Content and Thermal Fatigue Reliability of a Large Plastic Ball Grid Array (PBGA) Package," *Journal of SMT*, Vol. 24, Issue 1, 27-33, January-March 2011.

[34] Richard Coyle, Michael Reid, Claire Ryan, Richard Popowich, Peter Read, Debra Fleming, Maurice Collins, Jeff Punch, and Indraneel Chatterji, "The Influence of the Pb free Solder Alloy Composition and Processing Parameters on Thermal Fatigue Performance of a Ceramic Chip Resistor," *Proceedings of Electronic Components Technology Conference*, 423-430, IEEE, Piscataway, NJ 2009.

[35] J. Manock, R. Coyle, B. Vaccaro, H. McCormick, R. Popowich, D., P. Read., J. Osenbach, and D. Gerlach, “Effect of Temperature Cycling Parameters on the Solder Joint Reliability of a Pb-free PBGA Package,” *SMT J.*, vol. 21, no.3, 36, (2008).
[36] Richard Coyle, Peter Read, Steven Kummerl, Debra Fleming, Richard Popowich, and Indraneel Chatterji, “A Comprehensive Analysis of the Thermal Fatigue Reliability of SnPb and Pb Free Plastic Ball Grid Arrays (PBGA) Using Backward and Forward Compatible Assembly Processes,” *SMT J.*, Volume 21, Issue 4, 33-47, October-December 2008.
[37] M. Osterman, A. Dasgupta, and B. Han, “A Strain Range Based Model for Life Assessment of Pb-free SAC Solder Interconnects,” *Proceedings of Electronic Components and Technology Conference*, 884, IEEE, Piscataway, NJ (2006).
[38] J. Bath, S. Sethuraman, X. Zhou, D. Willie, K. Hyland, K. Newman, L. Hu, D. Love, H. Reynolds, K. Kochi, D. Chiang, V. Chin, S. Teng, M. Ahmed, G. Henshall, V. Schroeder, Q. Nguyen, A. Maheswari, M. Lee, J-P Clech, J. Cannis, J. Lau, C. Gibson, “Reliability Evaluations of Lead-Free SnAgCu PBGA676 Components Using Tin-Lead and Lead-Free SnAgCu Solder Paste,” *Proceedings of SMTAI*, 891, Edina, MN, (2005).
[39] S. Chaparala, B. Roggeman, J. Pitarresi, B. Sammakia, J. Jackson, G. Griffin, and T. McHugh, “Effect of Geometry and Temperature Cycle on the Reliability of WLCSP Solder Joints,” *IEEE Transactions on Components and Packaging Technologies*, Vol. 28, No. 3, 441-448, September 2005.
[40] J-P. Clech, “Acceleration Factors and Thermal Cycling Test Efficiency for Lead-free Sn-Ag-Cu Assemblies,” *Proceedings of SMTA International*, Chicago, IL, 902-917, 25-29 September 2005.
[41] X. Fan, G. Raiser, and V. Vasudevan, “Effects of Dwell Time and Ramp Rate on Lead-Free Solder Joints in FCBGA Packages,” *Electronic Components and Technology Conference*, 901-906, 2005.
[42] S.K. Kang, Paul Lauro, Da-Yuan Shih, Donald W. Henderson, Timothy Gosselin, Jay Bartelo, Steve R. Cain, Charles Goldsmith, Karl J. Puttlitz, and Tae-Kyung Hwang, “Evaluation of Thermal Fatigue Life and Failure Mechanisms of Sn-Ag-Cu Solder Joints with Reduced Ag Contents,” *Proceedings of Electronic Components and Technology Conference,* 661-667, Las Vegas, NV, 2004.
[43] J. Lee, and K. Subramanian, “Effect of Dwell Times on Thermomechanical Fatigue Behavior of Sn-Ag–Based Solder Joints,” *Journal of Electronic Materials*, Vol. 32, No. 6, 523- 530, 2003.
[44] J. Bartelo, S. Cain, D. Caletka, K. Darbha, T. Gosselin, D. Henderson, D. King, K. Knadle, A. Sarkhel, G. Thiel, C. Woychik, D. Shih, S. Kang, K. Puttlitz and J. Woods, “Thermomechanical Fatigue Behavior of Selected Pb-Free Solders, *Proceedings* of IPC APEX 2001, LF2-2, Bannockburn, IL, (2001).
[45] S. Yoon, Z. Chen, M. Osterman, B. Han, and A. Dasgupta, “Effect of Stress Relaxation on Board Level Reliability of Sn Based Pb-Free Solders,” *Proceedings of Electronic Components and Technology Conference*, Lake Buena Vista, FL, pp. 1210 – 1214, May 31 - June 3, 2005
[46] S. Dunford, S. Canumalla, and P. Viswanadham, “Intermetallic Morphology and Damage Evolution Under Thermomechanical Fatigue of Lead (Pb)-Free Solder Interconnections,” *Proceedings of Electronic Components Technology Conference,* 726-736, Las Vegas, NV, June 1-4, 2004.
[47] “Electronic Control Unit is at the Core of All Automotive Innovations: Know How the Story Unfolded,” Embitel Technologies, https://www.embitel.com/blog/embedded-blog/automotive-control-units-development-innovations-mechanical-to-electronics.
[48] R. Thompson, *Proc. SMTA/CAVE Workshop Harsh Environment Electronics*, Dearborn, MI, Jun. 24–25, 2003.
[49] M. R. Fairchild, R. B. Snyder, C. W. Berlin, and D. H. R. Sarma, “Emerging substrate technologies for harsh-environment automotive electronics applications,” *SAE Technical Paper Series 2002-01-1052*
[50] Anton-Zoran Miric, “New Developments In High-Temperature, High-Performance Lea d-Free Solder Alloys,” *SMTA Journal*, Volume 23, Issue 4, 24-29, 2010.
[51] H. Steen and B. Toleno, “Development of a Lead-Free Alloy for High-Reliability, High Temperature Applications,” *SMT*, January 2009.
[52] H-J Albrecht, P. Frühauf, and K. Wilke, “Pb-Free Alloy Alternatives: Reliability Investigation,” *Proceedings SMTAI 2009*, 308-316, San Diego, CA, 2009.
[53] J. Trodler, “Summary Innolot - Project March.2000 to February 2004,” W.C. Heraeus GmbH; CMD-AM-AT, Hanau, Germany, January 2009 (complete final report Confidential).
[54] J. Albrecht, “Final presentation BMBF project LIVE; Acceptance criteria of thermally highly stressed miniaturized solder joints,” Siemens AG, Corporate Technology, MM6, Berlin, Germany, September 17, 2008.
[55] Innovative Production Processes for High-temperature Electronics in Automotive Electronics Systems: Construction and Connection Technology, Volume 2, Mathias Nowottnick, Wolfgang Scheel, and Klaus Wittke, eds., 1st Edition, ISBN3-934142-52-4, M. Detert Publishing, Germany, May 2005.
[56] André Delhaise, Leonid Snugovsky, Doug Perovic, Polina Snugovsky, and Eva Kosiba, “Microstructure and Hardness of Bi-containing Solder Alloys after Solidification and Ageing,” SMTA J., Vol. 27, issue 3, 22-27, 2014.
[57] P.T. Vianco and J.A. Rejent, “Properties of Ternary Sn-Ag-Bi Solder Alloys: Part I - Thermal Properties and Microstructural Analysis,” J. Electronic Materials, Vol. 28, no. 10, 1127-1137, 1999.
[58] P.T. Vianco and J.A. Rejent, “Properties of Ternary Sn-Ag-Bi Solder Alloys: Part I - Wettability and Mechanical Properties Analyses,” J. Electronic Materials, Vol. 28, no. 10, 1138-1143, 1999.
[59] Jie Zhao˙ ,Lin Qi, Xiu-min Wang, “Influence of Bi on microstructures evolution and mechanical properties in Sn–Ag–Cu lead-free solder,” *J. Alloys and Compounds,* Vol. 375, Issues 1–2, 196-201, July 2004.
[60] Dave Hillman, Tim Pearson, and Ross Wilcoxon, “NASA DOD -55 ºC to +125 ºC Thermal Cycle Test

Results," *Proceedings of SMTAI 2010*, 512-518, Orlando, FL, October 2010.
[61] David Witkin, "Mechanical Properties of Bi-containing Pb-free Solders," *Proceedings IPC APEX 2013*, S11-01, San Diego, CA, February 2013.
[62] Joseph M. Juarez, Jr., Polina Snugovsky, Eva Kosiba, Zohreh Bagheri, Subramaniam Suthakaran, Michael Robinson, Joel Heebink, Jeffrey Kennedy, and Marianne Romansky, Manufacturability and Reliability Screening of Lower Melting Point Pb-Free Alloys Containing Bismuth, J. Microelectronics and Electronic Packaging," Vol. 12, no. 1, 1-28, 2015.
[63] Takatoshi Nishimura, Keith Sweatman, Akira Kita, Shuhei Sawada, "A New Method of Increasing the Reliability of Lead-Free Solder, *Proceedings of SMTAI 2015*, 736-742, Rosemont, IL, October 2015
[64] Amkor Technology Datasheets: CABGA DS550T (Rev. 11/15) and CTBGA DSS550N (Rev. 1/07), Amkor Technology, www.amkor.com, Tempe, AZ.
[65] W. Engelmaier, "The use environments of electronic assemblies and their impact on surface mount solder attachment reliability," *IEEE Trans. Components, Hybrids, and Manufacturing Technology,* vol. 13, no.4, 903-908, December 1990.
[66] S.A. Belyakov, B. Arfaei, C. Johnson, K. Howell, R. Coyle, and C.M. Gourlay, "Phase Formation and Solid Solubility in High Reliability Pb-free Solders Containing Bi, Sb or In," *Proceedings of SMTA International*, 492-506, September 22-26, 2019, Rosemont, IL.
[67] S.A. Belyakov, K. Sweatman, T. Akaiwa, T. Nishimura and C.M. Gourlay, "Precipitation of Bi and SbSn Phases in Next-Generation Pb-Free Solders," *Proceedings of SMTA International*, 484-491, September 22-26, 2019, Rosemont, IL.
[68] T. Wada, K. Mori, S. Joshi, and R. Garcia, "Superior Thermal Cycling Reliability of Pb-Free Solder Alloy by Addition of Indium and Bismuth for Harsh Environments, *Proceedings of SMTAI*, 210-215, Rosemont, IL, Sep 2016.
[69] T. Wada, S. Tsuchiya, S. Joshi, and R. Garcia, K. Mori, and T. Shirai, "Improving Thermal Cycle Reliability and Mechanical Drop Impact resistance of a Lead-free Tin-Silver-Bismuth-Indium Solder Alloy with Minor Doping of Copper Additive," *Proceedings of IPC APEX*, San Diego, CA, February 14-16, 2017.
[70] S.A. Belyakov, R.J. Coyle, B. Arfaei,3,4 J.W. Xian, and C.M. Gourlay, "Microstructure and Damage Evolution During Thermal Cycling of Sn-Ag-Cu Solders Containing Antimony," *Journal of Electronic Materials*, Vol. 50, No. 3, 2021. https://doi.org/10.1007/s11664-020-08507-x
[71] David Witkin, "Creep Behavior of Bi-Containing Lead-Free Solder Alloys," *Journal of Electronic Materials*, vol. 41, no. 2, 190-203, 2012.
[72] David B. Witkin, "Influence of microstructure on quasi-static and dynamic mechanical properties of bismuth-containing lead-free solder alloys,", Materials Science and Engineering A, vol. 532, 212-220, 2012.
[73] Alan M. Russell and Kok Loong Lee, Structure-Property Relation In Nonferrous Metals, John Wiley & Sons Publishing, 2005, ISBN-13 978-0-471-64952-6.
[74] I. J. Polmear, LIGHT ALOYS: Metallurgy of the Light Metals, 3.5.2 Al-Cu-Mg alloys (2xxx series) and 3.5.4 Al-Zn-Mg alloys (7xxx series) Halstead Press, John Wiley & Sons, Inc.,

Appendix A (Figure 1)

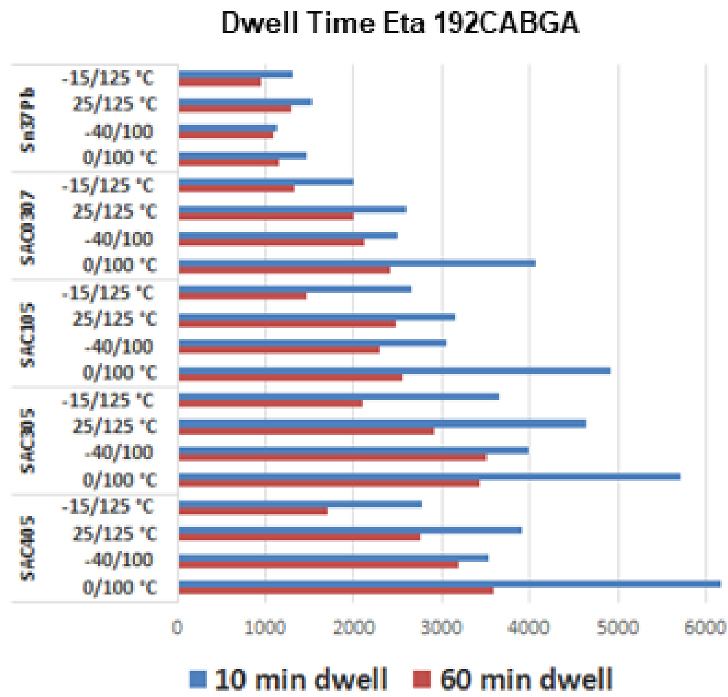

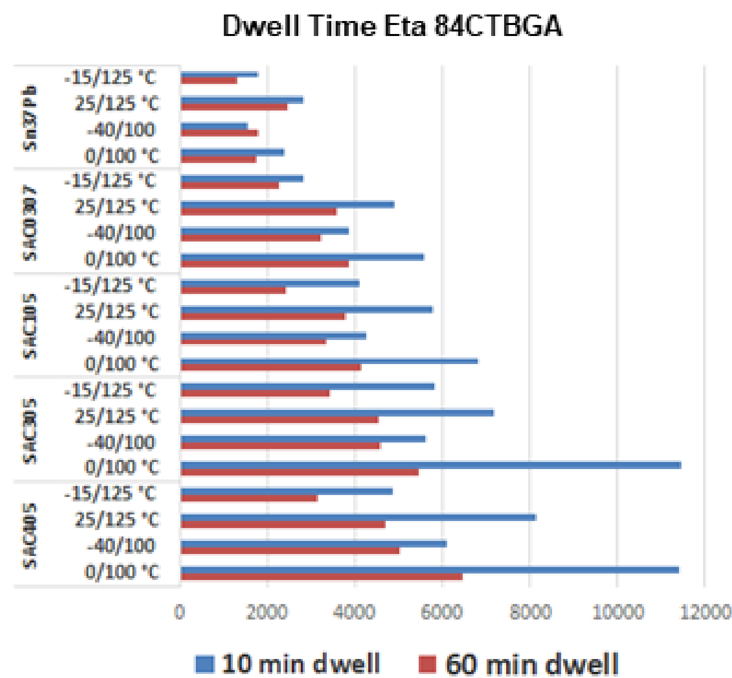

Figure 1. Bar charts illustrating the reduction in reliability with 60-minute dwell times from the alloy Alternatives project [12].

Appendix B (Figure 3)

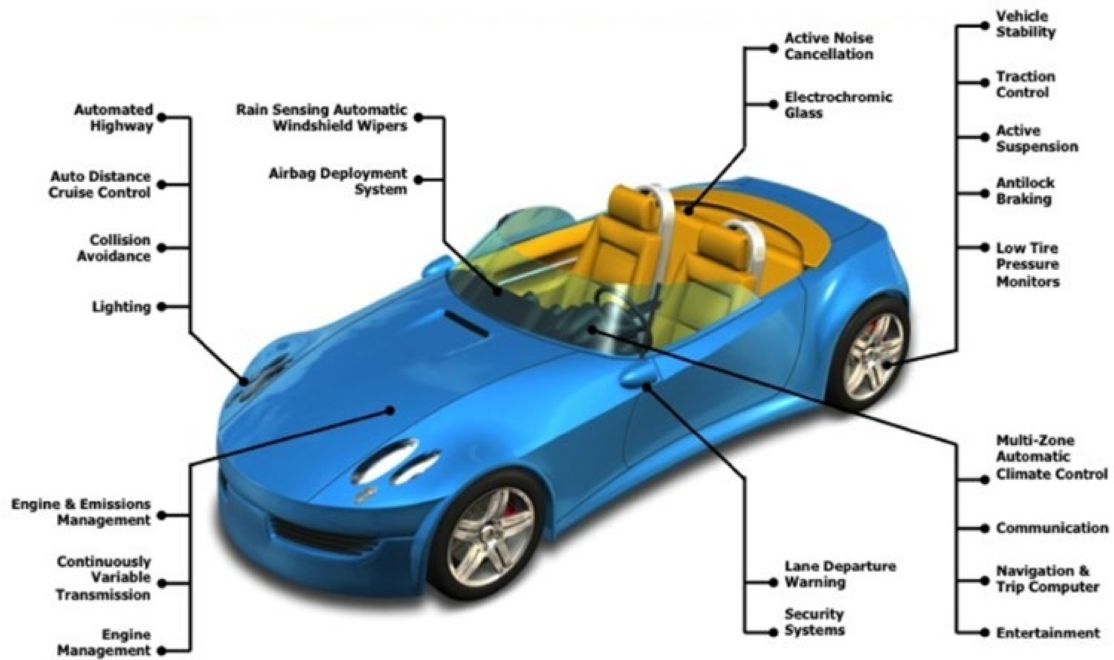

Figure 3. The proliferation of automotive sensors and electronic control modules [47].

Appendix C (Figure 4)

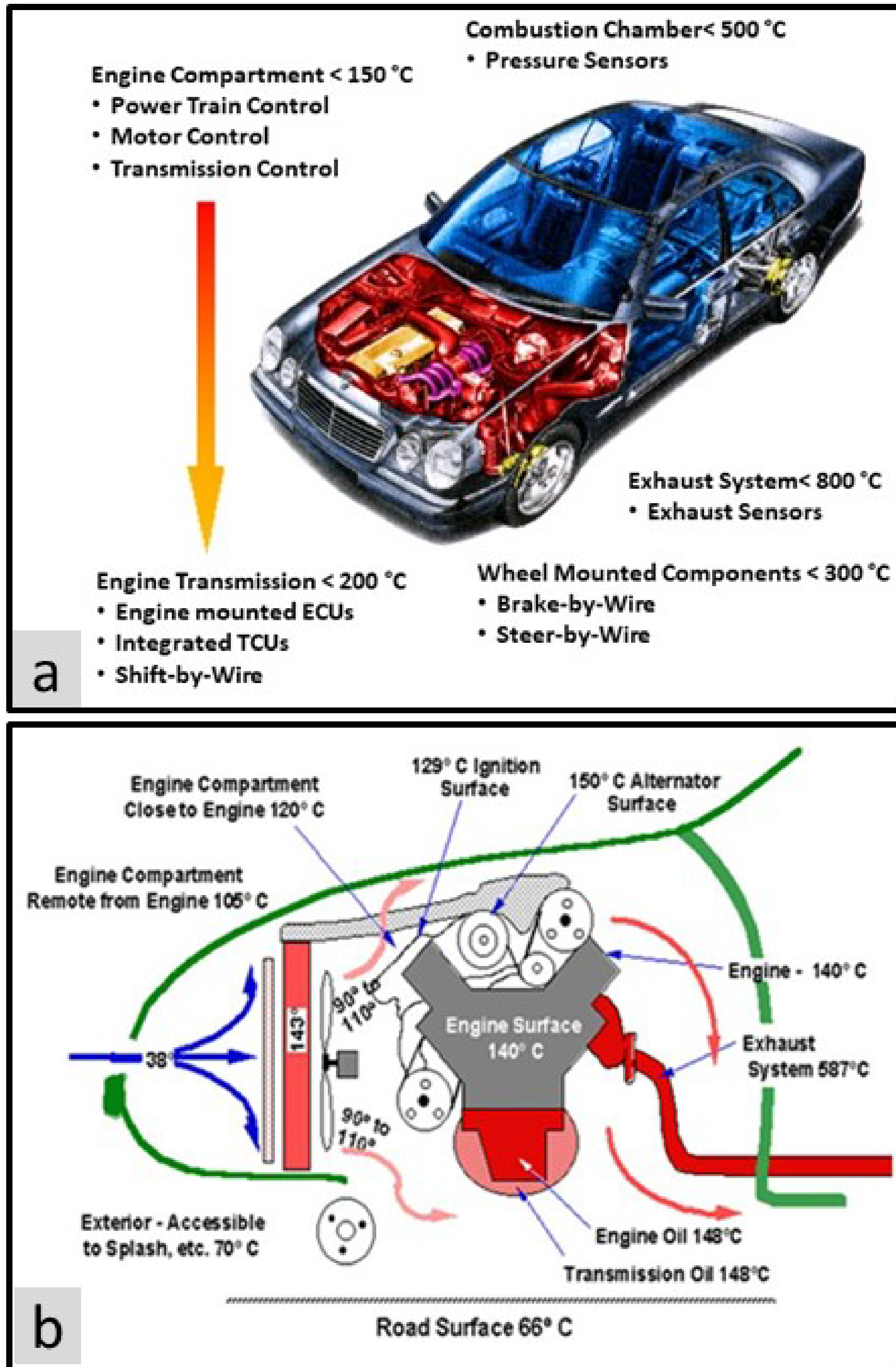

Figure 4. Illustrations of a) electronic control modules, sensor locations, and anticipated thermal exposures [48] and b) an engine compartment thermal profile [49].

Appendix D

Metallurgical Considerations for High-Performance Solder Alloys

Silver (Ag) Additions to Tin (Sn)

The addition of Ag strengthens Sn and improves the creep resistance of the SAC solder by precipitation hardening with Ag_3Sn precipitates as shown in Figure 1.

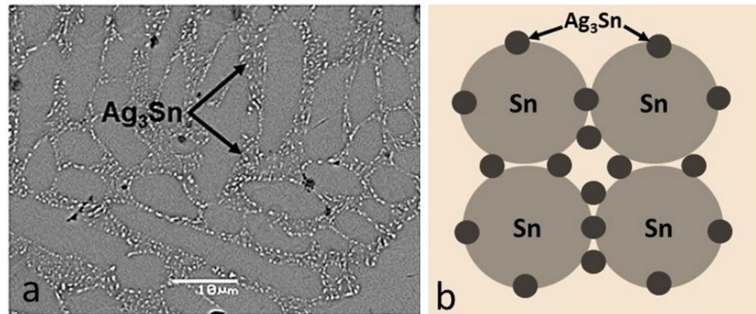

Figure 1. Precipitation hardening in SAC305 solder, a) backscattered scanning electron micrograph showing Ag_3Sn intermetallic precipitates, and b) schematic representation of Ag_3Sn precipitates along Sn dendrites.

The addition of other alloying elements can improve the creep resistance of the solder by means of two other well-known metallurgical strengthening mechanisms, solid solution hardening and dispersion hardening. The introduction of solute atoms into solid solution of a solvent-atom lattice invariably produces an alloy that is stronger than the pure metal [D1].

Figure 2 shows a simplified schematic illustration of substitutional solid solution strengthening. Substitutional or interstitial solute atoms strain the lattice and dislocation movement, or deformation is inhibited by interaction between dislocations and solute atoms incorporated into the β-Sn lattice.

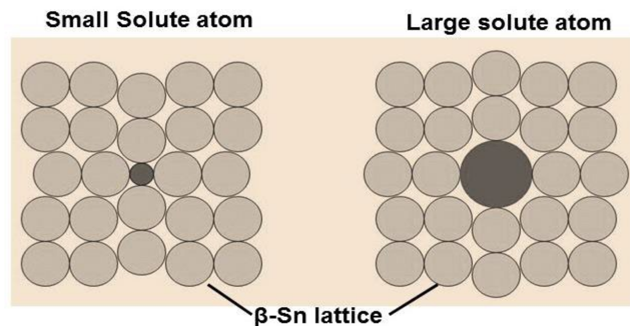

Figure 2. A simple schematic illustrating lattice distortion due to substitutional solute atoms.

If solute atoms precipitate from solution during thermal excursions in service, the solder alloy may strengthen subsequently due to dispersion hardening. Dispersion strengthening occurs when insoluble particles are finely dispersed in a metal matrix (Figure 3). Typical dispersion strengthened alloys employ an insoluble, incoherent second phase that is thermally stable over a large temperature range [D2]. For Sn-based solder alloys, the strength would be derived from a combination of increased solid solution strengthening at higher temperatures due to increased solubility, and dispersion strengthening that would supplement the solid solution effect at lower temperatures where solubility has decreased.

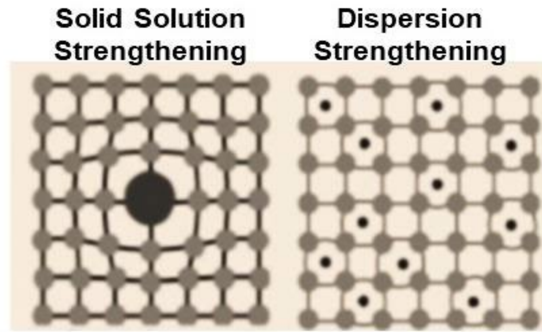

Figure 3. A simple schematic comparing solid solution (left) and dispersion strengthening (right).

The development of the alloy designated Innolot provides evidence that substitutional solid solution strengthening can improve resistance to creep and fatigue at higher temperatures in Sn- based, Pb-free solders [D3]. The current hypothesis is that solid solution and dispersion strengthening not only supplement the Ag_3Sn precipitate hardening found in SAC solders but continue to be effective once precipitate coarsening reduces the effectiveness of the intermetallic Ag_3Sn precipitates [D4].

The elements proposed most for improving elevated temperature properties in Sn-based, third generation solders are Bi, Sb and In. Bi and In, when used as major alloying elements, also reduce the melting point of most solder alloy formulations, while the addition of Sb tends to increase the melting point [3]. These modified SAC alloys are off-eutectic compositions and are characterized by non-equilibrium solidification and often significant melting ranges [D5-D8].

Antimony (Sb) Additions to Tin (Sn)

The binary Sn-Sb phase diagram in Figure 4 shows solubility of Sb in Sn of approximately 0.5 wt. % at room temperature to 1.5 wt. % at 125 ºC [D9, D10]. Thus, some contribution is expected from solid solution strengthening due to Sb dissolved in Sn-based Pb-free solders [D3].

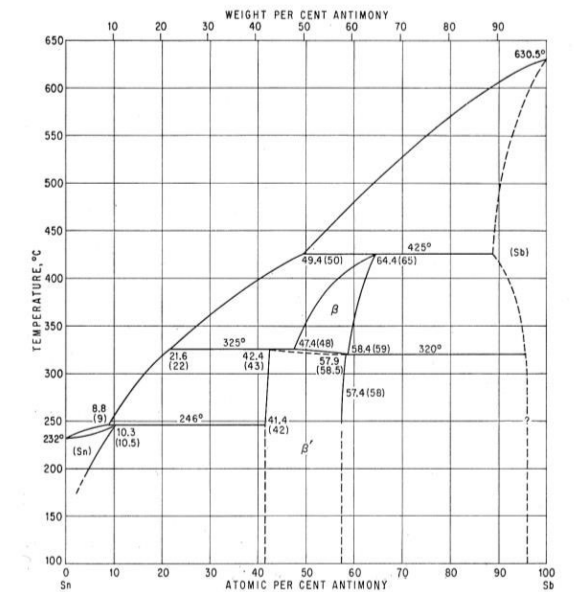

Figure 4. The Sn-Sb binary phase diagram [9].

Alloying with Sb may improve performance through other strengthening mechanisms. Studies by Li et al show that Sb slows the growth rate of Cu_6Sn_5 intermetallic compound (IMC) layers at attachment interfaces [D11, D12]. Fast interfacial IMC growth on Cu surfaces tends to produce irregular and non-

uniform IMC layers. This can lead to reduced mechanical reliability by inducing fractures at IMC interfaces or through the IMC in drop/shock loading [D13].

Figure 4 also shows that Sb has the potential to form multiple different intermediate phases or IMCs with Sn (Sb_2Sn_3, SbSn, Sb_4Sn_3, Sb_5Sn_4, and $SbSn_2$) in the bulk solder. Lu et al [D14] and El-Daly et al [D15] identified SnSb intermediate phase precipitates < 5µm in size and distributed throughout the Sn dendrites. Beyer et al show that Sn5Sb and Sn8Sb alloys have increased shear strength and ductility compared to conventional SAC solders and maintain their shear strength with good ductility after isothermal aging [D16]. El-Daly suggests Sb also can improve creep performance and tensile strength [D17].

In this case, the SbSn precipitates form within the Sn dendrites, unlike the well-known SAC Ag_3Sn mechanism, where the precipitates form at the Sn dendrite boundaries. It is assumed, the SbSn precipitates work to resist recrystallization by strengthening the Sn dendrites [D18].

Indium (In) Additions to Tin (Sn)

The binary Sn-In phase diagram in shown in Figure 5. While there is some disagreement over the solid solubility of In in Sn, a reasonable estimate is ~7 wt. % at room temperature and as much as 12 wt. % at 125 °C [D19]. Because of its range of solubility in Sn, In has been explored as a solid solution strengthening agent in Sn-based Pb-free solders [D20, D21]. The equilibrium diagram shows that indium forms two intermediate phases (β and γ) of variable composition with Sn [D19] but does not appear to form any true stoichiometric compounds with Sn.

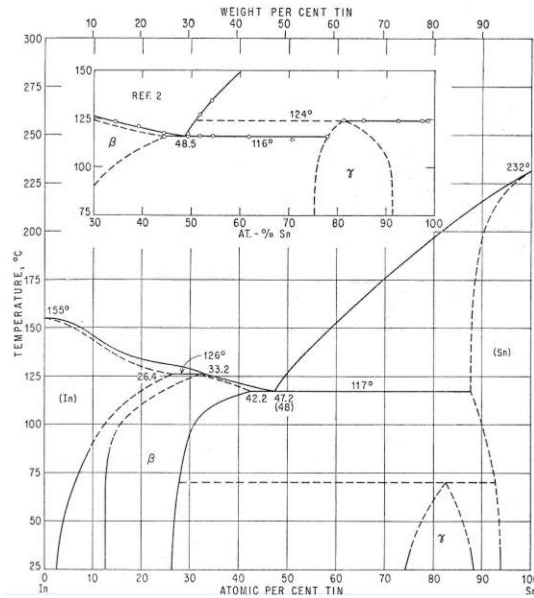

Figure 5. The In-Sn binary phase diagram [D19].

Results from multiple solder alloy studies indicate that In additions can improve drop and shock resistance by slowing the growth of interfacial IMC layers. Yu et al report improved drop [D22] and thermal shock [D23] performance by adding as little as 0.4% In, and Amagai et al report improved drop performance at or below 0.5 % In [D24]. Hodúlová et al In slows growth of Cu_3Sn and that a hybrid IMC phase $Cu_6(Sn, In)_5$ forms [D25]. Sharif also observed the formation of the $Cu_6(Sn, In)_5$ IMC as well as formation of $(Cu, Ni)_3(Sn, In)_4$ on Ni substrates [-26], and these IMCs also could be found in the bulk as well as the interfaces. In these hybrid IMCs, In substitutes for Sn which fundamentally is different than the common modified IMCs $(Cu, Ni)_6Sn_5$ or the $(Ni, Cu)_3Sn_4$ where Cu and Ni exchange.

Other reactions can occur when In is added to SAC-based solders, and this complicates the ability to understand the effect of In content on solder joint reliability. In a study by Chantaramanee et al additions of 0.5% In or Sb in combination with In was found to promote formation of $Ag_3(Sn, In)$ and SnSb [D27]. They reported that small precipitates reduced the Sn dendrite size by 28%, but they were unable to determine the relative influence of In versus Sb on this reaction. With alloys containing In of the order of 10 %, Sopoušek et al found that some of the Ag_3Sn

transforms to $Ag_2(Sn,In)$ and Ag_2Sn [D28]. These observations are consistent with the Ag-Sn binary phase diagram that shows Ag_3In, Ag_2In, and $AgIn_2$ [D29]. Wang et al reported that an addition of 1% In caused larger or coarser Ag_3Sn precipitates [D30]. This is an interesting observation, since Ag_3Sn precipitate coarsening (larger precipitates at time zero) could reduce thermal cycling reliability. In principle there is a large solid solubility of In in Sn, but the effective In content in a SAC-based solder may be diminished by interactions with other elements to form multiple phases.

It is noteworthy that many of the studies were conducted using laboratory bulk solder samples with microstructures that are likely to be atypical of microelectronic solder joints. Some of the studies also included more than one significant alloy addition [e.g., D27], which makes it difficult to isolate effects due to individual alloying elements. The work by Wada et al [20, 21], while it includes tensile testing with comparatively large, bulk samples, also includes thermal cycling and drop testing with surface mount components. Their microstructural analysis included X-ray diffraction and they found $InSn_4$, In_4Ag_9, $Ag_3(Sn, In)$, and possibly αSn in addition to βSn. Wada concluded that the optimum ductility and reliability was achieved with an In content of 6 wt. %.

Bismuth (Bi) Additions to Tin (Sn)

The binary Sn-Bi phase diagram in shown in Figure 6. The solubility of Bi in Sn is approximately 1.5 wt. % at room temperature and increases to almost 7 wt. % at 100 ºC room temperature, and as much as 15 wt. % at 125 ºC [D31]. There is minimal solubility of Sn in Bi, and no intermediate phases or IMC are found in the Sn-Bi system.

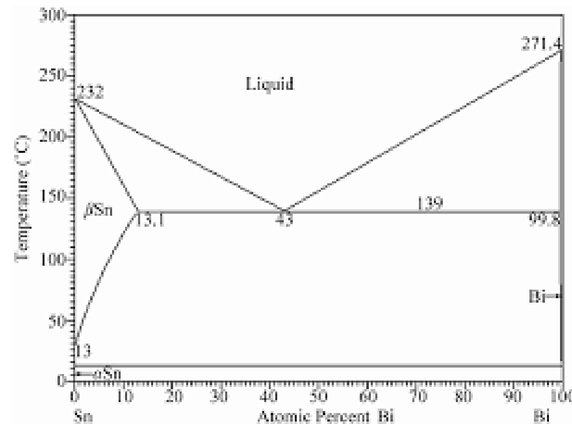

Figure 6. The Sn-Bi binary phase diagram [D31].

Multiple studies have shown that Bi improves the mechanical properties of Sn and SAC solders [D3, D32, D33-D40, D41-D46]. Vianco [D34, D35] and Witkin [D42-D44] have done extensive mechanical testing and microstructural analysis and discuss the dual strengthening mechanisms of Bi in solid solution and Bi precipitated within Sn dendrites and at Sn boundaries. Recently, Delhaise et al [D68] reported results from their study of the effects of thermal preconditioning (aging) on microstructure and property improvement in an alloy containing 6 wt. % Bi (see Table 1, Violet). They suggest that strain from Bi precipitation induces recrystallization and an increase in the amount of Sn grain boundaries which in turn, are pinned by the Bi precipitates at those boundaries. These microstructural features work in conjunction with Bi in solid solution to resist creep deformation.

The results from the fundamental studies by Vianco [D34, D35] and Witkin [D42-D44] leave no doubt that Bi additions can have a positive effect on the physical properties of Sn and Sn-based solder alloys. However, those studies used cast, bulk alloy samples and it is debatable if those results can be scaled effectively to smaller, microelectronic solder joints. Nishimura et al for example, recommend a maximum Bi content of only 1.5 wt. % (Figure 7a) because of the uncertainly that the alloying effect will be sustained as the microstructure evolves in response to the thermal cycling in normal service [D40]. Delhaise has shown that the Bi distribution and microstructure depend on solidification conditions and subsequent thermal exposure, which determine the relative contributions of Bi to solid solution and dispersion strengthening (Figure 7b) [D45]. Furthermore, it is possible that adding enough Bi to take advantage of the Bi solubility limit at higher temperatures may have a negative effect

because Bi does not always precipitate homogeneously. Clustering of Bi is known to occur [D45] and in the extreme case, stratification or segregation may induce brittle behavior [D47, D48].

The current experimental test plan offers the opportunity to explore the stability of the Bi content in the Violet alloy using thermal cycling at upper temperature extremes of 100 °C and 125 °C.

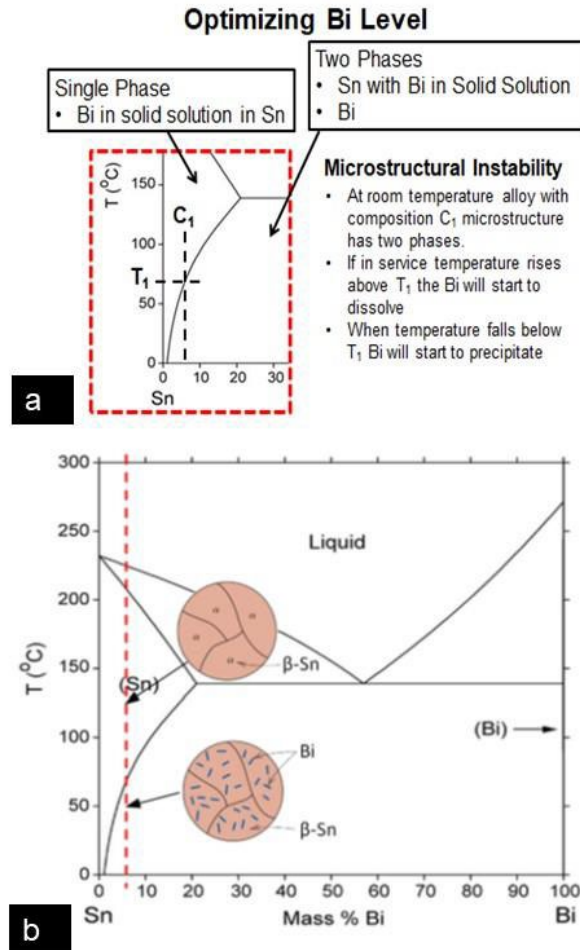

Figure 7. Emphasis on the Sn-rich regions of the Sn-Bi binary phase diagram showing a) Factors to consider when for optimizing the Bi level, courtesy, K. Sweatman [D46], and b) Microstructures shown schematically for solid solution (upper) and dispersion strengthening (lower) with the 6 wt. % Bi alloy (Violet), from Delhaise [D45].

References

[D1] G. E. Dieter, Mechanical Metallurgy, Chapter 5, "Plastic Deformation of Polycrystalline Aggregates, Solid Solution Hardening," 128, McGraw-Hill, 1961.

[D2] Peter Haasen, Physical Metallurgy, 3rd Edition, Cambridge University Press, 375-378, 1996.

[D3] Anton-Zoran Miric, "New Developments In High-Temperature, High-Performance Lea d-Free Solder Alloys,"
SMTA Journal, Volume 23, Issue 4, 24-29, 2010.

[D4] André Delhaise, Leonid Snugovsky, Doug Perovic, Polina Snugovsky, and Eva Kosiba, "Microstructure and Hardness of Bi-containing Solder Alloys after Solidification and Ageing," SMTA J., Vol. 27, issue 3, 22-27, 2014.

[D5] "Lead-Free Solder Project Final Report," *NCMS Report 0401RE96, Section 2.4, Properties Assessment and Alloy Down Selection,* National Center for Manufacturing Sciences, Ann Arbor, MI, May 1997.

[D6] T. Siewert, S. Liu, D. R. Smith, and J. C. Madeni, "Database for Solder Properties with Emphasis on New Lead-Free Solders: Properties of Lead-Free Solders Release 4.0," NIST and Colorado School of Mines, February 2002.

[D7] C. A. Handwerker, E. E. de Kluizenaar, K. Suganuma, and F. W. Gayle, "Major International Lead (Pb)-Free Solder Studies," Chapter 17, in Karl J. Puttlitz and Kathleen. A. Stalter, eds., Handbook of

Lead-Free Solder Technology for Microelectronic Assemblies, 665-728, Marcel Dekker, New York, 2004.
[D8] C. A. Handwerker, U. Kattner, K. Moon, J. Bath, and P. Snugovsky, “Chapter 1, Alloy Selection,” in Lead-Free Electronics, 9-46, IEEE Press, Piscataway, NJ, 2007.
[D9] Max Hansen, Constitution of Binary Alloys, 2nd edition, McGraw-Hill, 1175-1177, 1958.
[D10] Rodney P. Elliot, Constitution of Binary Alloys, First Supplement, McGraw-Hill, 802, 1965.
[D11] Li, G.Y., Chen, B.L., Tey, J.N., “Reaction of Sn-3.5Ag-0.7Cu-xSb solder with Cu metallization during reflow soldering,” *IEEE Transactions on Electronics Packaging Manufacturing*, vol. 27, no. 1, 77-85, 2004.
[D12] Li, G.Y., Bi, X.D., Chen, Q., Shi, X.Q., “Influence of dopant on growth of intermetallic layers in Sn-Ag-Cu solder joints,” *Journal of Electronic Materials,* vol. 40, no. 2,165-175, 2011.
[D13] Per-Erik Tegehall “Review of the Impact of Intermetallic Layers on the Brittleness of Tin-Lead and Lead-Free Solder Joints, Section 3, Impact of Intermetallic Compounds on the Risk for Brittle Fractures” *IVF Project Report 06/07*, IVF Industrial Research and Development Corporation, 2006.
[D14] Lu, S., Zheng, Z., Chen, J., Luo, F., “Microstructure and solderability of Sn-3.5Ag-0.5Cu-xBi-ySb solders,”
Proceedings 11th International Conference on Electronic Packaging Technology and High Density Packaging, ICEPT-HDP 2010, 410-412, 2010.
[D15] A.A. El-Daly, Y. Swilem and A.E. Hammad, “Influences of Ag and Au Additions on Structure and Tensile Strength of Sn-5Sb Lead Free Solder Alloy,” *J. Mater. Sci. Technol*., vol.24, no. 6, 921-925, 2008.
[D16] H. Beyer, V. Sivasubramaniam, D. Hajas, E. Nanser, F. Brem, “Reliability improvement of large area soldering connections by antimony containing lead-free solder,” *PCIM Europe Conference Proceedings*, 1069-1076, 2014.
[D17] A.A. El-Daly, Y. Swilem, A.E. Hammad, “Creep properties of Sn–Sb based lead-free solder alloys,” *Journal of Alloys and Compounds*, vol. 471, 98-104, 2009.
[D18] G. E. Dieter, Mechanical Metallurgy, Chapter 6, “Dislocation Theory” 159, McGraw-Hill, 1961.
[D19] Max Hansen, Constitution of Binary Alloys, 2nd edition, McGraw-Hill, 860-863, 1958.
[D20] T. Wada, K. Mori, S. Joshi, and R. Garcia, “Superior Thermal Cycling Reliability of Pb-Free Solder Alloy by Addition of Indium and Bismuth for Harsh Environments, *Proceedings of SMTAI*, 210-215, Rosemont, IL, Sep 2016.
[D21] T. Wada, S. Tsuchiya, S. Joshi, and R. Garcia, K. Mori, and T. Shirai, “Improving Thermal Cycle Reliability and Mechanical Drop Impact resistance of a Lead-free Tin-Silver-Bismuth-Indium Solder Alloy with Minor Doping of Copper Additive,” *Proceedings of IPC APEX*, San Diego, CA, February 14-16, 2017.
[D22] A-M Yu, J-W Jang, J-H Lee, J-K Kim, M-S Kim, “Microstructure and drop/shock reliability of Sn-Ag-Cu-In solder joints,” *International Journal of Materials and Structural Integrity*, vol. 8 no. 1-3, 42-52, 2014.
[D23] A-M Yu, J-W Jang, J-H Lee, J-K Kim, M-S Kim, “Tensile properties and thermal shock reliability of Sn-Ag-Cu solder joint with indium addition,” *Journal of Nanoscience and Nanotechnology*, vol. 12, no. 4, 3655-3657, 2012.
[D24] M. Amagai, Y. Toyoda, T. Ohnishi, S. Akita, “High drop test reliability: Lead-free solders,” *Proceedings 54th Electronic Components and Technology Conference*, 1304-1309, 2004.
[D25] E. Hodúlová, M. Palcut, E. Lechovič, B. Šimeková, K. Ulrich, “Kinetics of intermetallic phase formation at the interface of Sn-Ag-Cu-X (X = Bi, In) solders with Cu substrate,” *Journal of Alloys and Compounds*, vol. 509, no. 25, 7052-7059, 2011.
[D26] A. Sharif, Y. C. Chan, “Liquid and solid state interfacial reactions of Sn-Ag-Cu and Sn-In-Ag-Cu solders with Ni-P under bump metallization,” *Thin Solid Films*, vol. 504, no. 1-2, 431-435, 2006.
[D27] S. Chantaramanee, P. Sungkhaphaitoon, T. Plookphol, “Influence of indium and antimony additions on mechanical properties and microstructure of Sn-3.0Ag-0.5Cu lead free solder alloys,” *Solid State Phenomena*, 266 SSP, 196-200, 2017.
[D28] J. Sopoušek, M. Palcut, E. Hodúlová, J. Janovec, “Thermal analysis of the Sn-Ag-Cu-In solder alloy,” *Journal of Electronic Materials*, vol. 39, no. 3, 312-317, 2010.
[D29] Max Hansen, Constitution of Binary Alloys, 2nd edition, McGraw-Hill, 26-28, 1958.
[30] J. Wang, M. Yin, Z. Lai, X. Li, “Wettability and microstructure of Sn-Ag-Cu-In solder,” Hanjie Xuebao/Transactions of the China Welding Institution, vol. 32, no. 11, 69-72, 2011.
[D31] Max Hansen, Constitution of Binary Alloys, 2nd edition, McGraw-Hill, 336-339, 1958.
[D32] Polina Snugovsky, Simin Bagheri, Marianne Romansky, Doug Perovic, Leonid Snugovsky, and John Rutter, “New Generation Of Pb-Free Solder Alloys: Possible Solution To Solve Current Issues With Main Stream Pb-Free Soldering,” SMTA J., Vol. 25, issue 3, 42-52, July 2012.
[D33] André Delhaise, Leonid Snugovsky, Doug Perovic, Polina Snugovsky, and Eva Kosiba, “Microstructure and Hardness of Bi-containing Solder Alloys after Solidification and Ageing,” SMTA J., Vol. 27, issue 3, 22-27, 2014.

[D34] P.T. Vianco and J.A. Rejent, “Properties of Ternary Sn-Ag-Bi Solder Alloys: Part I - Thermal Properties and Microstructural Analysis,” J. Electronic Materials, Vol. 28, no. 10, 1127-1137, 1999.

[D35] P.T. Vianco and J.A. Rejent, “Properties of Ternary Sn-Ag-Bi Solder Alloys: Part I - Wettability and Mechanical Properties Analyses,” J. Electronic Materials, Vol. 28, no. 10, 1138-1143, 1999.

[D36] Jie Zhao, ,Lin Qi, Xiu-min Wang, “Influence of Bi on microstructures evolution and mechanical properties in Sn–Ag–Cu lead-free solder,” *J. Alloys and Compounds,* Vol. 375, Issues 1–2, 196-201, July 2004.

[D37] Dave Hillman, Tim Pearson, and Ross Wilcoxon, “NASA DOD -55 ºC to +125 ºC Thermal Cycle Test Results,” *Proceedings of SMTAI 2010*, 512-518, Orlando, FL, October 2010.

[D38] David Witkin, “Mechanical Properties of Bi-containing Pb-free Solders,” *Proceedings IPC APEX 2013*, S11-01, San Diego, CA, February 2013.

[D39] Joseph M. Juarez, Jr., Polina Snugovsky, Eva Kosiba, Zohreh Bagheri, Subramaniam Suthakaran, Michael Robinson, Joel Heebink, Jeffrey Kennedy, and Marianne Romansky, Manufacturability and Reliability Screening of Lower Melting Point Pb-Free Alloys Containing Bismuth, J. Microelectronics and Electronic Packaging,” Vol. 12, no. 1, 1-28, 2015.

[D40] Takatoshi Nishimura, Keith Sweatman, Akira Kita, Shuhei Sawada, “A New Method of Increasing the Reliability of Lead-Free Solder, *Proceedings of SMTAI 2015*, 736-742, Rosemont, IL, October 2015

[D41] A. Delhaise, L. Snugovsky, D. Perovic, P. Snugovsky, E. Kosiba, The Effects of Bi and Ageing on the Microstructure and Mechanical Properties of Sn-rich Alloys, Pt. 2, 2016 International Conference on Soldering & Reliability, Toronto, Canada, May 9-11, 2016.

[D42] David Witkin, Mechanical Properties of Bi-containing Pb-Free Solders, APEX Expo 2013, San Diego, CA, February 16-21, 2013

[D43] David Witkin, “Creep Behavior of Bi-Containing Lead-Free Solder Alloys,” *Journal of Electronic Materials*, vol. 41, no. 2, 190-203, 2012.

[D44] David B. Witkin, “Influence of microstructure on quasi-static and dynamic mechanical properties of bismuth-containing lead-free solder alloys,”, Materials Science and Engineering A, vol. 532, 212-220, 2012.

[D45] André M. Delhaise, Polina Snugovsky, Ivan Matijevic, Jeff Kennedy, Marianne Romansky, David Hillman, David Adams, Stephan Meschter, Joseph Juarez, Milea Kammer, Ivan Straznicky, Leonid Snugovsky, Doug D. Perovic, “Thermal Preconditioning, Microstructure Restoration and Property Improvement in Bi-Containing Solder Alloys,” *SMTA Journal*, vol. 31, issue1, 33-42, 2018

[D46] Keith Sweatman, Nihon Superior, private communication, November 2017.

[D47] C. H. Raeder, L. E. Felton, D. B. Knott, G. B. Shmeelk and D. Lee, “Microstructural Evolution and Mechanical Properties of Sn-Bi based Solders,” *Proceedings of International Electronics Manufacturing Technology Symposium,* 119-127, Santa Clara, CA, October 1993.

[D48] Richard Coyle, Raiyo Aspandiar, Michael Osterman, Charmaine Johnson, Richard Popowich, Richard Parker, Dave Hillman, “Thermal Cycle reliability of a Low Ag Ball Grid Array Assembled with Tin Bismuth Solder paste,” *Proceedings of SMTAI*, 108-116, Rosemont, IL, September 17-21, 2017.

Appendix E (Figure 5)

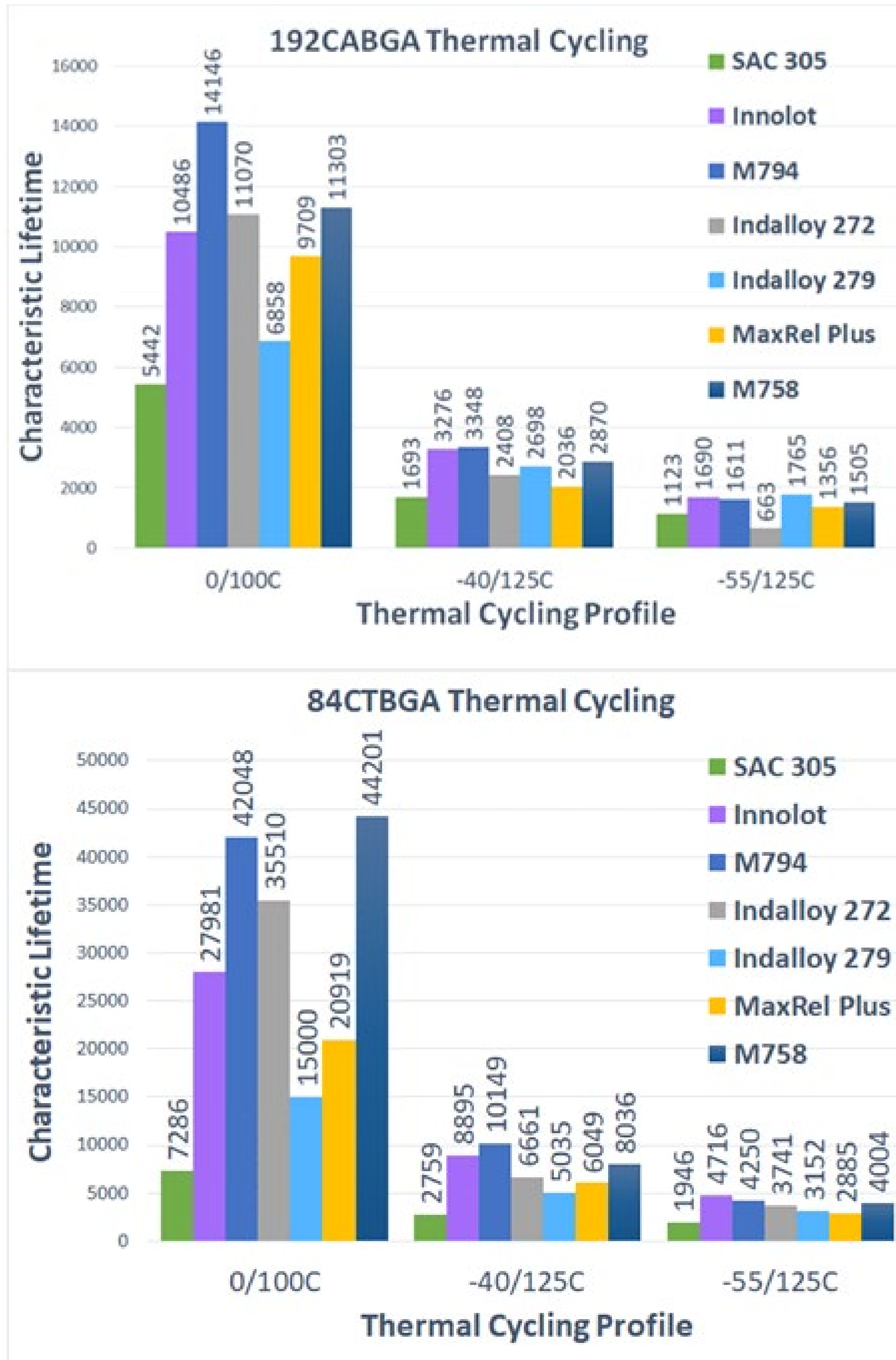

Figure 5. Bar charts comparing the characteristic lifetimes for the 192CABGA and 84CTBGA with SAC305 and the five high-performance solder alloys tested with the 0/100 °C, -40/125 °C and -55/125 °C thermal cycling profiles.

Appendix F (Figure 6)

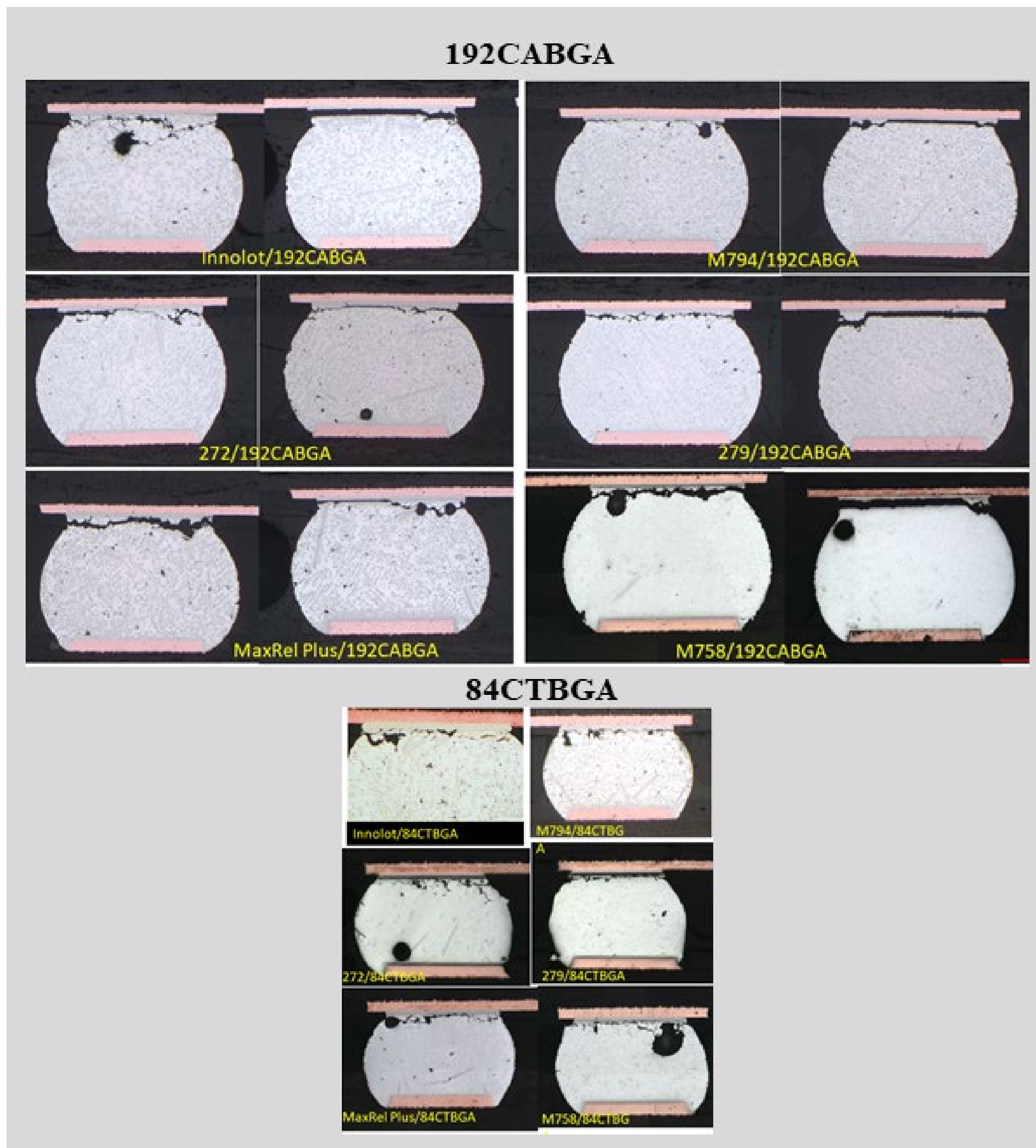

Figure 6. Optical photomicrographs showing examples of thermal fatigue damage and interfacial fracturing in the solder joints of the 192CABGA for all the high-performance solder alloys (upper), and solder fatigue damage only in the solder joints of the 84CTBGA for all high-performance alloys. SAC305 exhibits only fatigue damage with both components. The thermal cycling test profile was -55/125 °C (TC4).

Appendix G
iNEMI Lead-Free Alloy Alternatives BGA Thermal Cycling Test Vehicle

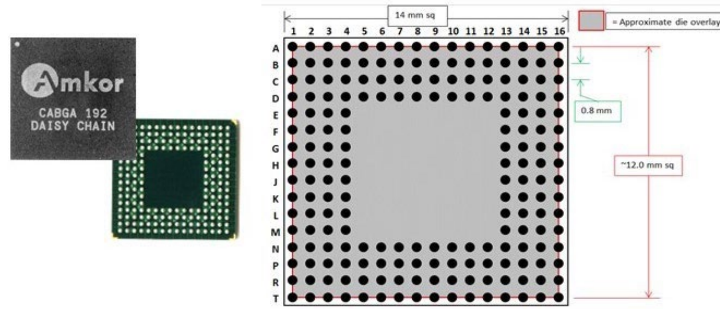

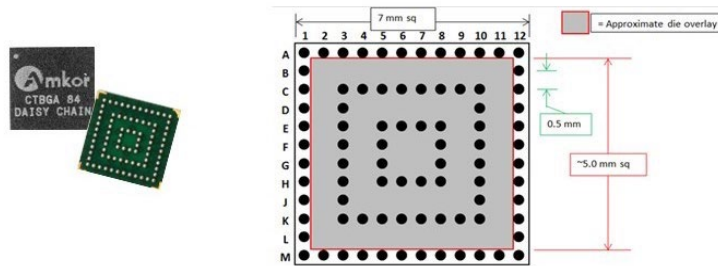

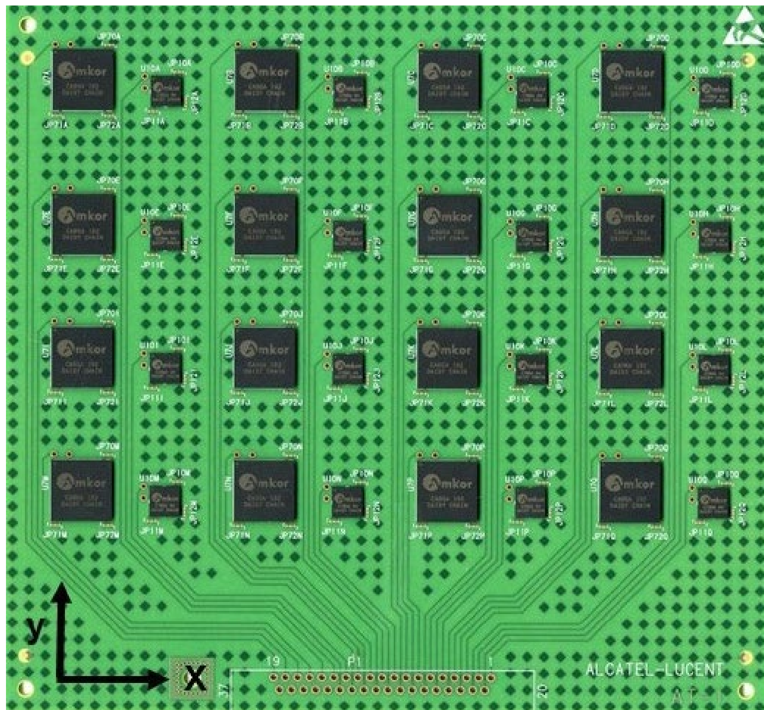

Appendix H

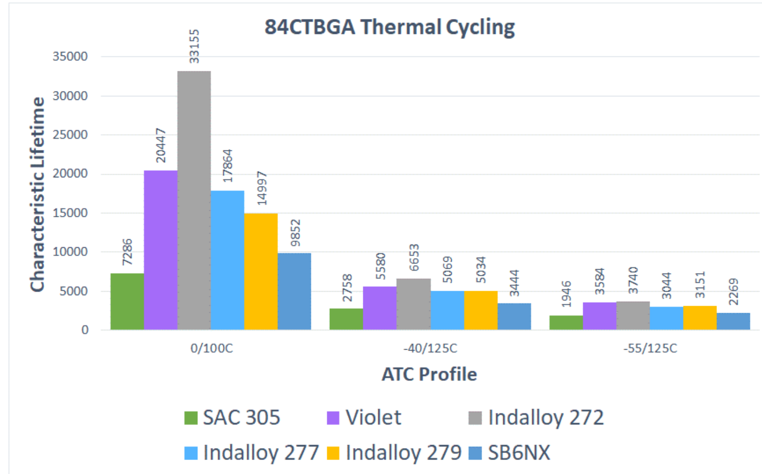

Figure 9. Bar charts comparing the characteristic lifetimes for the 84CTBGA with SAC305, and five high-performance solder alloys tested with the 0/100 °C, -40/125 °C and -55/125 °C thermal cycling profiles [26].